THE PLANT CELL

The Plant Cell, 2024, **36**, 4457–4471

https://doi.org/10.1093/plcell/koae200
Advance access publication 12 July 2024
Research Article

PHOSPHATASE 2A dephosphorylates PHYTOCHROME-INTERACTING FACTOR3 to modulate photomorphogenesis in Arabidopsis

Xingbo Cai,[1] Sanghwa Lee,[1,†] Andrea Paola Gómez Jaime,[1] Wenqiang Tang,[2] Yu Sun,[2] Enamul Huq[1,*]

[1]Department of Molecular Biosciences and the Institute for Cellular and Molecular Biology, The University of Texas at Austin, Austin, TX 78712, USA
[2]Key Laboratory of Molecular and Cellular Biology of Ministry of Education, College of Life Sciences, Hebei Normal University, Shijiazhuang, Hebei 050024, China
*Author for correspondence: huq@austin.utexas.edu
[†]Present address: Plant Molecular and Cellular Biology Laboratory, Salk Institute for Biological Studies, 10010 N Torrey Pines Rd, La Jolla, CA 92037, USA.
The author(s) responsible for distribution of materials integral to the findings presented in this article in accordance with the policy described in the Instructions for Authors (https://academic.oup.com/plcell/pages/General-Instructions) is: Enamul Huq (huq@austin.utexas.edu).

Abstract

The phytochrome (phy) family of sensory photoreceptors modulates developmental programs in response to ambient light. Phys also control gene expression in part by directly interacting with the bHLH class of transcription factors, PHYTOCHROME-INTERACTING FACTORS (PIFs), and inducing their rapid phosphorylation and degradation. Several kinases have been shown to phosphorylate PIFs and promote their degradation. However, the phosphatases that dephosphorylate PIFs are less understood. In this study, we describe 4 regulatory subunits of the Arabidopsis (*Arabidopsis thaliana*) protein PHOSPHATASE 2A (PP2A) family (B′α, B′β, B″α, and B″β) that interact with PIF3 in yeast 2-hybrid, in vitro and in vivo assays. The *pp2ab″αβ* and *b″αβ/b′αβ* mutants display short hypocotyls, while the overexpression of the B subunits induces longer hypocotyls compared with the wild type (WT) under red light. The light-induced degradation of PIF3 is faster in the *b″αβ/b′αβ* quadruple mutant compared with that in the WT. Consistently, immunoprecipitated PP2A A and B subunits directly dephosphorylate PIF3-MYC in vitro. An RNA-sequencing analysis shows that B″α and B″β alter global gene expression in response to red light. *PIFs* (*PIF1*, *PIF3*, *PIF4*, and *PIF5*) are epistatic to these B subunits in regulating hypocotyl elongation under red light. Collectively, these data show an essential function of PP2A in dephosphorylating PIF3 to modulate photomorphogenesis in Arabidopsis.

IN A NUTSHELL

Background: Light is not only an important energy source for photosynthesis, but also a crucial informational signal that regulates plant development throughout the life cycle. The phytochrome (phy) family of sensory photoreceptors perceives ambient light signal and transduces this signal to control nuclear gene expression in part by directly interacting with the transcription factors called the PHYTOCHROME-INTERACTING FACTORS (PIFs). Phytochromes induce rapid phosphorylation and degradation of PIFs by recruiting several kinases. However, the phosphatases that dephosphorylate PIFs under light remain less investigated.

Question: Is there any phosphatase(s) that dephosphorylate PIF3 and other PIFs under light to regulate its abundance and/or activity?

Findings: In this study, we describe the identification of four regulatory subunits of the Arabidopsis protein phosphatase 2A (PP2A) family (B′α, B′β, B″α and B″β) that regulate PIF3 phosphorylation status to modulate photomorphogenesis in Arabidopsis. These four B subunits interacted with PIF3 in several in vitro and in vivo assays. Phenotypic analyses showed that the four B subunits promote hypocotyl elongation specifically under red light. The B subunits inhibit the degradation of PIF3 by directly dephosphorylating PIF3. The gene expression analysis and epistatic analysis support a conclusion where the B subunits promote hypocotyl elongation by stabilizing PIF3 under red light.

Next steps: The results in this study suggest that there are additional phosphatases that might regulate PIF abundance and/or activity. In addition, the specific dephosphorylation sites are still unknown. Identifying additional phosphatases and the specific dephosphorylation sites will enhance our understanding of how phosphatases regulate PIF abundance and/or activity to fine tune photomorphogenesis.

Received April 09, 2024. Accepted July 2, 2024

Introduction

Plants employ a battery of sensory photoreceptors for perceiving and responding to the surrounding light environment (Bae and Choi 2008). The phytochrome (phy) family, which is encoded by 5 genes in Arabidopsis (*Arabidopsis thaliana*) (*PHYA-PHYE*) perceives and responds to the red/far-red region of the light spectrum and controls development throughout the plant life cycle (Legris et al. 2019; Cheng et al. 2021). Upon exposure to red light, phys change conformation from an inactive Pr form to an activated Pfr form. The activated Pfr form is translocated from the cytoplasm into the nucleus and interacts with multiple nuclear proteins. Among those, the PHYTOCHROME-INTERACTING FACTORs (PIFs), a small family of basic helix–loop–helix (bHLH) transcription factors, are primary interacting partners as they specifically bind to the Pfr form (Leivar and Quail 2011; Pham et al. 2018b; Huq et al. 2024). PIFs function primarily as negative regulators of photomorphogenesis to repress seed germination, promote hypocotyl elongation, and display shade avoidance responses (Lee and Choi 2017; Pham et al. 2018b). To remove these negative regulators, light-activated phys induce rapid phosphorylation, ubiquitination, and degradation of PIFs through the 26S proteasome pathway to promote photomorphogenesis (Pham et al. 2018b; Cheng et al. 2021; Cai and Huq 2024). In addition, phys also interact with PIFs and inhibit the DNA binding and transcriptional activation activity of PIFs in response to light (Park et al. 2012, 2018; Yoo et al. 2021; Huq et al. 2024).

In recent years, multiple E3 ubiquitin ligases and kinases involved in PIF degradation have been described (Cheng et al. 2021). Two E3 ligase complexes have been reported to promote PIF3 degradation, the Light-Response-Bric-a-Brack/Tramtrack/Broad (LRB)-CULLIN3 complex (Ni et al. 2014) and the EIN3-BINDING F BOX PROTEIN (EBF)-CULLIN1 complex (Dong et al. 2017). The LRB E3 ligase mediates the codegradation of PIF3 and phyB in response to light, while the EBF1/2 E3 ligase has no effect on phyB stability. SUPPRESSOR OF PHYA-105 1 family members (SPA1 to SPA4) directly interact with the E3 ligase CONSTITUTIVELY PHOTOMORPHOGENIC1 and function as a cognate kinase-E3 ligase complex to mediate light-induced degradation of PIF1 to promote seed germination and seedling development (Zhu et al. 2015; Pham et al. 2018a; Paik et al. 2019). CASEIN KINASE2 (CK2) directly phosphorylates PIF1 in a light-independent manner. However, the CK2-mediated phosphorylation of PIF1 is necessary for the light-induced degradation of PIF1 (Bu et al. 2011b). PHOTOREGULATORY PROTEIN KINASES (PPK1 to PPK4) interact with and phosphorylate PIF3 in a light-inducible fashion (Ni et al. 2017) and induce PIF3-phyB codegradation. In addition, the MAP kinase MPK6 has been shown to phosphorylate PIF3 and regulate its turnover (Xin et al. 2018). Interestingly, SALT OVERLY SENSITIVE2 phosphorylates PIF1 and PIF3 to promote their degradation under salt stress conditions, while it phosphorylates PIF4 and PIF5 to stabilize them under shade conditions (Han et al. 2023; Ma et al. 2023). However, PIFs are degraded not only in light but also under dark conditions. The GSK3-like kinase BRASSINOSTEROID-INSENSITIVE2 (BIN2) phosphorylates both PIF3 and PIF4 and promotes their degradation in dark conditions (Bernardo-García et al. 2014; Ling et al. 2017; Huq et al. 2024).

A reversible phosphorylation of phys as well as phy signaling partners plays a crucial role in light signaling pathways. For example, the phosphorylation of phys regulates their interaction with signaling partners (Choi et al. 1999; Kim et al. 2004; Nito et al. 2013), as well as dark reversion of phyB (Medzihradszky et al. 2013). The catalytic subunit of Arabidopsis PROTEIN PHOSPHATASE2A (PP2A) (FLOWER-SPECIFIC, PHYTOCHROME-ASSOCIATED PROTEIN PHOSPHATASE3, AtFyPP3) interacts with, and dephosphorylates, oat (*Avena sativa*) phyA to regulate flowering time (Kim et al. 2002). PHYTOCHROME-ASSOCIATED PROTEIN PHOSPHATASE5 (PAPP5) specifically dephosphorylates the Pfr form of phys and enhances phy signaling (Ryu et al. 2005). PAPP2C directly dephosphorylates phys and indirectly mediates the in vitro dephosphorylation of PIF3 (Phee et al. 2008). Only 2 phosphatases, TYPE-1 PROTEIN PHOSPHATASE4 (TOPP4, a catalytic subunit of PP1) and FyPP1/FyPP2 (catalytic subunits of PP6), have been shown to dephosphorylate PIF3 to PIF5 and regulate their abundance (Yue et al. 2016; Yu et al. 2019). However, FyPP1/2 mainly functions in the dark to repress photomorphogenesis. Although TOPP4 dephosphorylates the light-induced phosphorylated form of PIF5, the TOPP4 mutant is a dwarf mutant, suggesting a more general function in regulating seedling growth. Thus, the phosphatases that function as bona fide light signaling components are still unclear.

PP2A is a group of ubiquitous and highly conserved serine-threonine phosphatases, involved in the growth and development and phytohormone signaling pathways in plants (Luan 2003; Farkas et al. 2007; Booker and DeLong 2017; Bheri et al. 2021). In Arabidopsis, functional PP2A is a heterotrimeric complex, consisting of a scaffolding A subunit (3 isoforms), a catalytic C subunit (5 isoforms), and a regulatory B subunit (18 isoforms). The A and C subunits act as core enzymes, while the B subunit determines substrate specificity and subcellular localization of the ABC trimer. The catalytic subunits of PP2A and other SERINE/THREONINE-SPECIFIC PHOSPHOPROTEIN PHOSPHATASE (PPP) family members are conserved due to a high sequence similarity. Also, the 3 A subunits show similar functions because of their high amino acid sequence similarity. Unlike the conserved A and C subunits, the members of the B subunit exist in different gene families. In Arabidopsis, B subunits are further divided into B, B′, and B″ subfamilies. The spatiotemporal gene expression and subcellular localization of these subunits are involved in determining the substrate specificity and enzymatic activity of the PP2A family (Farkas et al. 2007).

In an effort to isolate phosphatases that are involved in the dephosphorylation of PIFs, we identify 4 regulatory subunits of PP2A (B′α, B′β, B″α, and B″β) that interact with PIF3 in vitro and in vivo. We show that B′α, B′β, B″α, and B″β delay the red-light-induced PIF3 degradation and promote hypocotyl elongation specifically under red-light conditions. Thus, PP2A regulatory subunits act as negative regulators of phyB signaling by dephosphorylating PIF3 and preventing PIF3 degradation.

Results

PIF3 interacts with PP2A B′α, B′β, B″α, and B″β in vivo and in vitro

To identify the potential phosphatases that interact with PIFs, we performed a yeast 2-hybrid (Y2H) screening using PIF3 as a bait. We identified 4 regulatory subunits of the PP2A family of phosphatases (B′α, B′β, B″α, and B″β) that interact with PIF3 (Fig. 1A; Supplementary Fig. S1A). B′α and B′β belong to the B′ subfamily, and B″α and B″β are from the B″ subfamily with a high sequence similarity (Supplementary Fig. S2, A and B). However, there is a low sequence similarity among all 4 subunits (Supplementary Fig. S2C), and the B′ and B″ form distinct clades in a phylogenetic tree (Farkas et al. 2007; Wang et al. 2016). B′α and B′β have been reported to dephosphorylate BZR1 to activate brassinosteroid-responsive gene expression and plant growth in Arabidopsis (Tang et al. 2011). B″α and B″β interact with HMGR1S and

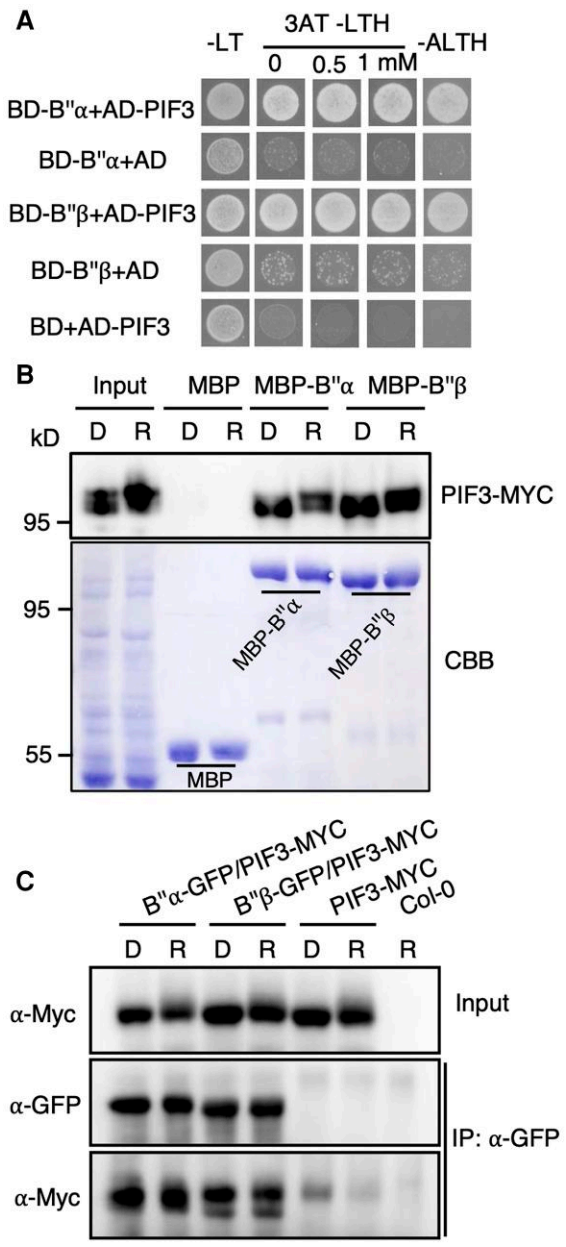

Figure 1. PIF3 interacts with PP2A B″α and B″β in vitro and in vivo. **A)** Y2H assays of the interaction between full-length PIF3 and PP2A B″α and B″β subunits. The B″α- and B″β-GAL4-DNA-binding domain (BD-B″α and BD-B″β) fusion was coexpressed with the GAL4-activation domain (AD) fused to full-length PIF3 or AD by itself as a negative control. Yeast cells were grown on selective media lacking histidine, supplemented with an increasing concentration of the histidine biosynthesis inhibitor 3-amino triazole (3-AT). **B)** A semi-in vivo pull-down assay shows the interaction between PIF3-MYC and MBP-B″α and MBP-B″β. MBP-B″α and MBP-B″β proteins were incubated with extracts from 4-d-old dark-grown seedlings of the PIF3-MYC transgenic line (dark- or red-light treated) and then were pulled down by MBP beads. Finally, PIF3-MYC signals were detected by a-Myc. MBP only as a negative control. Inputs from dark- and red-light-treated extracts as positive controls. **C)** An in vivo co-IP assay shows that PIF3-MYC interacts with B″α-GFP and B″β-GFP in response to red light or in dark conditions. Four-day-old dark-grown seedlings of 35s:B″α-GFP/PIF3-MYC, 35s:B″β-GFP/PIF3-MYC, PIF3-MYC, and Col-0 were used. PIF3-MYC and Col-0 were used as negative controls. All the seedlings were treated with 100 μM Bortezomib for 4 h in darkness. One batch was kept in the dark condition and the other batch was treated with red light. An a-GFP antibody was used to immunoprecipitate B″α-GFP and B″β-GFP and an a-MYC antibody was used to detect the PIF3-MYC protein. CBB, Coomassie brilliant blue stain; D, dark; R, red light.

HMGR1L, the major isoforms of 3-hydroxy-3-methylglutaryl-CoA reductase (HMGR) in Arabidopsis, in a Ca^{2+}-inducible manner, and PP2A mediates the regulation of HMGR in transcript, protein, and activity levels in response to stress conditions (Leivar et al. 2011). Because PP2A is a heterotrimeric complex in plants, we examined whether PIF3 also interacts with the A and C subunits. However, no interaction was detected between PIF3 and PP2A A and C subunits (Supplementary Fig. S3).

To verify the interactions between PIF3 and B subunits, a semi-in vivo pull-down assay was performed. B″α and B″β fused with the maltose-binding protein (MBP) were used to incubate with the extracts from dark- and light-exposed seedlings of the 35S-promoter-driven *PIF3-MYC* overexpression line, and the MBP beads were used to pull down the MBP protein and then detect PIF3-MYC signals. As shown in Fig. 1B, the PIF3-MYC signals were detected from dark- or red-light-treated conditions. Furthermore, co-immunoprecipitation (co-IP) was conducted by using stable transgenic plants (*35S:B″α-GFP/35S:PIF3-MYC* and *35S:B″β-GFP/35S:PIF3-MYC*) to verify their interactions. As expected, B″α-GFP and B″β-GFP showed strong interactions with PIF3-MYC in vivo independent of light (Fig. 1C). We also performed Y2H interaction assays and semi-in vivo pull-down and co-IP experiments and found that PIF3 interacted with B′α and B′β (Supplementary Fig. S1, A to C). In summary, these results suggest that PP2A B′α, B′β, B″α, and B″β interact with PIF3 in vitro and in vivo.

Since major PIFs (PIF1, PIF3, PIF4, and PIF5) share high similarity within protein sequences and form homo- and heterodimers (Castillon et al. 2007; Bu et al. 2011a; Lee and Choi 2017), we tested whether other PIFs (PIF1, PIF4, and PIF5) could interact with PP2A B″α and B″β. Interestingly, we found that PP2A B″α and B″β could indeed interact with PIF1, PIF4, and PIF5 in yeast and in semi-in vivo pull-down experiments (Supplementary Fig. S4, A to D), suggesting that B″α and B″β interact with 4 major PIFs and may regulate their abundance.

PP2A B subunits promote hypocotyl elongation under red light

To examine whether PP2A B″α and B″β regulate photomorphogenesis, we first isolated T-DNA insertion lines of *b″α* (SALK_135978) and *b″β* (SALK_151964) and created overexpression lines using 35S-promoter-driven *B″α* and *B″β* fused with GFP at the C-terminus. Reverse transcription PCR (RT-PCR) assays confirmed that the expression of *B″α* and *B″β* was undetected in these mutants, respectively (Supplementary Fig. S5). Since PIF3 is involved in regulating hypocotyl elongation under red light (Kim et al. 2003; Monte et al. 2004), we examined the hypocotyl phenotype of the *pp2ab″α* and *b″β* single mutants and the overexpression lines under dark- and red-light conditions. We found that *pp2ab″α* and *b″β* exhibited shorter hypocotyl lengths specifically under red-light conditions compared with the Columbia-0 (Col-0) wild type (WT; Supplementary Fig. S6). To eliminate the redundancy involved, we generated the double mutant of *b″α* and *b″β* and then analyzed the hypocotyl phenotype. The *pp2ab″αβ* double mutant (or just called *b″αβ*) showed a shorter hypocotyl length compared with the WT (Fig. 2, A to D), similar to the *b″β* single mutant under red-light conditions (Supplementary Fig. S6). Conversely, the overexpression lines of B″α (*B″α-OX*) and B″β (*B″β-OX*) exhibited longer hypocotyls than those of the WT in red-light conditions but not in dark conditions (Fig. 2, E to H). However, the hypocotyl length of *b″αβ* was similar to that of the WT under darkness, suggesting that the role of PP2A B″α and B″β is red-light specific (Fig. 2,

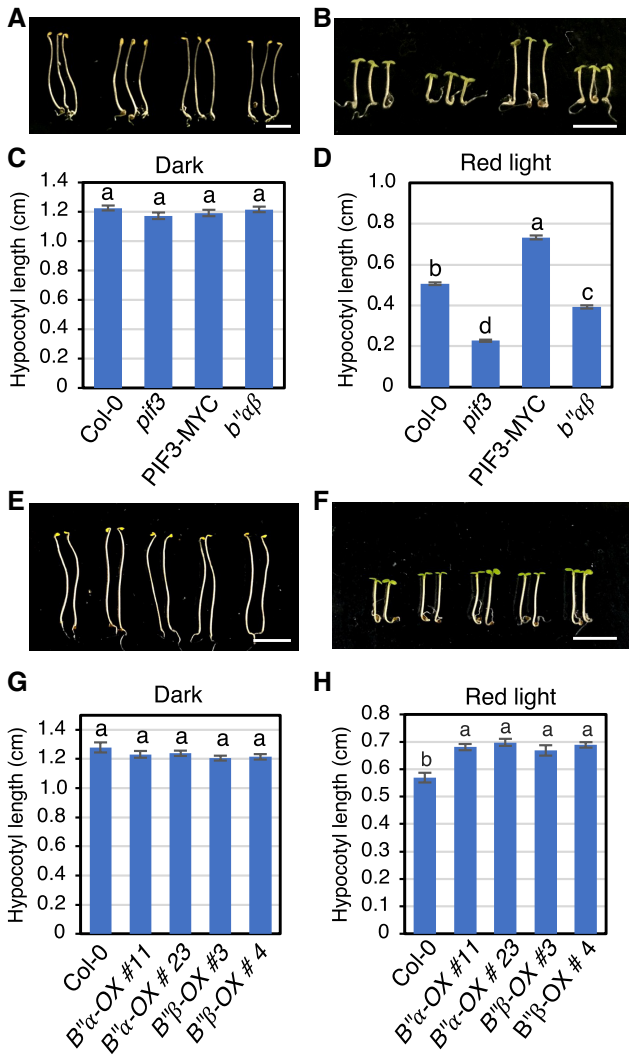

Figure 2. PP2A B″α and B″β promote hypocotyl elongation in red-light conditions. **A and B**) The photographs showing the seedling phenotypes of *pp2ab″αβ* grown in darkness **(A)** and red-light (8 μmol m^{-2} s^{-1}) conditions **(B)**, respectively, for 4 d. The seedling order in the image from left to right is: Col-0, *pif3*, PIF3-MYC, and *pp2ab″αβ*. Scale bar in **A** and **B**: 5 mm. **C and D)** The bar graphs show the hypocotyl lengths of seedlings shown in **A** and **B** ($n \geq 24$). The error bars represent SE. A 1-way ANOVA was performed. Statistically significant differences are indicated by different lowercase letters ($P < 0.05$). **E** and **F**) Photographs showing the seedling phenotypes of B″**α** overexpression lines (B″*α* #11 and #23) and B″*β* overexpression lines (B″*β* #3 and #4) grown in darkness **(E)** and red-light conditions (8 μmol m^{-2} s^{-1}), respectively, for 4 d. The seedling order in the image from left to right is: Col-0, B″**α** overexpression Lines #11 and #23, and B″*β* overexpression Lines #3 and #4. Scale bar in **E** and **F**: 5 mm. **G** and **H)** The bar graphs show the hypocotyl lengths of seedlings shown in **E** and **F** ($n \geq 10$). The error bars represent SE. A 1-way ANOVA was performed. Statistically significant differences are indicated by different lowercase letters ($P < 0.05$).

A and C; Supplementary Fig. S6). Intriguingly, the hypocotyl length of the *b″αβ* double mutant was not as short as that of the *pif3* mutant, suggesting that other phosphatases may be involved in this process.

To test whether *B′α* and *B′β* also function in photomorphogenesis, in the same way as *B″α* and *B″β*, we examined the hypocotyl phenotype of the *b′αβ* double mutant and the *B′α-OX* line. Similar to *b″αβ*, *b′αβ* exhibited short hypocotyls, while the *B′α-OX* line showed long hypocotyls under red-light conditions compared with the WT (Supplementary Fig. S7, A to H). Interestingly, *b′αβ* showed an even stronger hypocotyl phenotype than that of *b″αβ*. However, the *b′αβ* and *B′α-OX* lines exhibited a slightly shorter and longer hypocotyl phenotype compared with the WT under dark conditions, respectively (Supplementary Fig. S7, A to H), suggesting that B′**α** and B′**β** might also function in dark conditions, as has been shown previously (Tang et al. 2011). To test whether these 4 B subunits were functioning redundantly in regulating hypocotyl elongation, we crossed *b″αβ* and *b′αβ* and generated the *pp2ab″αβ/b′αβ* quadruple mutant. We found that the hypocotyl phenotype of *pp2ab″αβ/b′αβ* was as strong as that of *b′αβ* (Supplementary Fig. S7, A to D). Taken together, these data indicate that B subunits promote hypocotyl elongation under red-light conditions.

To test whether PP2A A subunits are involved in regulating photomorphogenesis, we generated 2 independent lines of the 35S-promoter-driven overexpression lines of RCN1 (*RCN1-OX*) and A3 (*A3-OX*) with a C-terminal GFP tag in a WT background and examined the hypocotyl elongation phenotype under the same condition. As expected, both *RCN1-OX* and *A3-OX* displayed longer hypocotyls in red-light conditions compared with the WT (Supplementary Fig. S8, A to D), indicating that PP2A A subunits also contribute to hypocotyl elongation. In summary, these data indicate that PP2A acts as a negative regulator of photomorphogenesis under red-light conditions.

PIFs and B″α and B″β function in the same genetic pathway to regulate hypocotyl elongation

Because B′**α**, B′**β**, B″**α**, B″**β**, and PIF3 regulated hypocotyl elongation, we tested whether B″**α**, B″**β**, and PIFs functioned in the same genetic pathway to regulate hypocotyl elongation. To answer this question, we generated *cr-pif3* and *cr-pif3 b″αβ* triple mutants by using CRISPR-Cas9 to mutate *PIF3* in the WT and *b″αβ* backgrounds. The immunoblot results showed no expression of the PIF3 protein in these *pif3* CRISPR lines (Supplementary Fig. S9E). There was no difference in hypocotyl length among genotypes, including WT and *cr-pif3b″αβ* triple mutants under dark conditions (Supplementary Fig. S9, A and C). However, under red-light conditions, all the *pif3* CRISPR lines in the WT background showed short hypocotyls compared with the WT (Supplementary Fig. S9, B and D). The triple mutant showed even shorter hypocotyls than the *pif3* CRISPR lines (Supplementary Fig. S9, B and D). To further explore the genetic relationship between PIFs and B″**α** and B″**β**, we crossed the *pif1pif3pif4pif5* quadruple mutant (*pifQ*) with *b″αβ* and generated the *pifQ/b″αβ* sextuple mutant and examined the hypocotyl lengths under dark and red-light conditions. The results showed that *pifQ* and the *pifQ/b″αβ* sextuple mutant exhibited the same hypocotyl length in both dark- and red-light conditions (Fig. 3, A to D), suggesting that *pifQ* is epistatic to *b″αβ*.

To further confirm the genetic relationship between *PIF3* and *B″β*, *35S:B″β-GFP/pif3* was generated and the hypocotyl length measured. The results showed that the long hypocotyl phenotype of *B″β-OX* was largely eliminated in the *B″β-OX/pif3* background under red-light conditions (Fig. 3, E to H), indicating that the *B″β-OX* phenotype is mostly PIF3 dependent. However, the hypocotyl length of *B″β-OX/pif3* was still slightly longer than that of *pif3*, suggesting that *B″β-OX* might be acting on other PIFs. This was consistent with the interaction of B″**β** with other PIFs (Supplementary Fig. S4). An immunoblot analysis confirmed that B″**β**-GFP protein levels were not different between the Col-0 and the *pif3* backgrounds (Supplementary Fig. S10, A and B), indicating that the PIF3 mutation causes the short hypocotyl length of *B″β-OX/pif3*

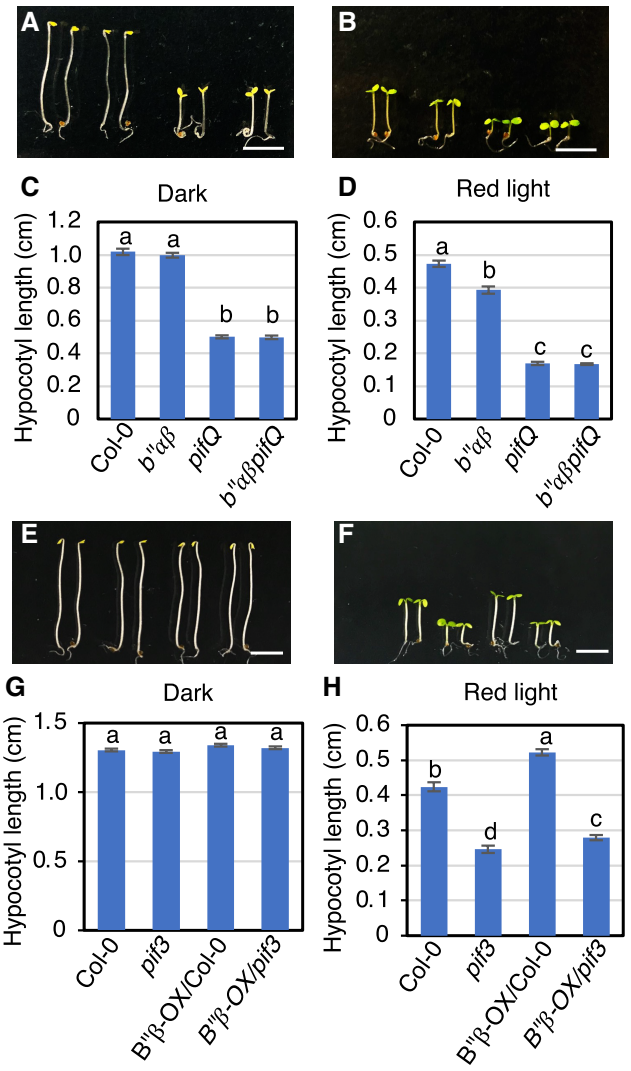

Figure 3. PP2A B″α and B″β and PIFs act in the same genetic pathway to regulate hypocotyl elongation in *Arabidopsis*. **A** and **B)** Photographs showing the seedling phenotypes grown in darkness **(A)** and red-light conditions (**B**, 8 μmol m^{-2} s^{-1}), respectively, for 4 d. The seedling order in the image from left to right is: Col-0, *pp2ab″αβ*, *pifQ*, and *b″αβpifQ*. Scale bar in **A** and **B**: 5 mm. **C** and **D)** The bar graphs exhibit the hypocotyl lengths of seedlings shown in **A** and **B** ($n \geq 30$). The error bars represent SE. A 1-way ANOVA was performed. Statistically significant differences are indicated by different lowercase letters ($P < 0.05$). **E** and **F**) Photographs showing the seedling phenotypes grown in darkness **(A)** and red-light conditions (**B**, 8 μmol m^{-2} s^{-1}), respectively, for 4 d. The seedling order in the image from left to right is: Col-0, *pif3*, *B″β-OX/Col-0*, and *B″β-OX/pif3*. Scale bar in **A** and **B**: 5 mm. **G** and **H)** The bar graphs display the hypocotyl lengths of seedlings shown in **E** and **F** ($n \geq 20$). The error bars represent SE. A 1-way ANOVA was performed. Statistically significant differences are indicated by different lowercase letters ($P < 0.05$).

and not the protein level of B″β-GFP. These data demonstrate that PIFs and both B″α and B″β function in the same genetic pathway to regulate hypocotyl elongation under red light.

To provide additional genetic evidence, we also used the CRISPR-Cas9 method to mutate *B″α* and *B″β* simultaneously in the *35S:PIF3-MYC* background. We identified 1 *35S:PIF3-MYC/cr-b″αβ* #32 line. The sequencing results revealed that this line contained 1 bp deletion in *B″α* and 1 bp insertion in *B″β* (Supplementary Fig. S11A), which caused frame shifts and led to early termination (Supplementary Fig. S11, B and C). A phenotypic analysis showed that *35S:PIF3-MYC/cr-b″αβ* #32 exhibited shorter hypocotyls than *35S:PIF3-MYC* under red-light conditions (Supplementary Fig. S12), suggesting that B″α and B″β promote PIF3 function, possibly by inhibiting a red-light-induced degradation of PIF3.

To substantiate these genetic data, we used a pharmacological approach and treated the WT, *pif3*, *35S:PIF3-MYC*, and *b″αβ* double mutants and *B″α-OX* and *B″β-OX* seedlings with cantharidin, a widely used inhibitor of PP1 and PP2A (Honkanen 1993) under red light and checked the hypocotyl length. As shown in Supplementary Figs. S13A and S14A, with the increasing concentration of cantharidin, the hypocotyl elongation was gradually inhibited among all the genotypes. Fifteen micromolars cantharidin could abolish the long hypocotyl phenotype of *35S:PIF3-MYC*, *B″α-OX*, and *B″β-OX* under red-light conditions. The relative hypocotyl length change was calculated by using hypocotyl length values from a 15 μM cantharidin condition divided by the values of DMSO control, and the results revealed that *pif3* and *pifQ* displayed hyposensitivity to cantharidin (Supplementary Figs. S13B and S14B). The *b″αβ* double mutant and *b″αβ/b′αβ* quadruple mutant were less sensitive to cantharidin treatment compared with the WT (Supplementary Figs. S13B and S14B). However, *35S:PIF3-MYC*, *B″α-OX*, and *B″β-OX* were hypersensitive to cantharidin (Supplementary Fig. S13B). These data suggest that PP2A or possibly PP1 activity is critical for the longer hypocotyl phenotype of *35S:PIF3-MYC*, *B″α-OX*, and *B″β-OX* under red light.

PP2A dephosphorylates and stabilizes PIF3 from red-light-induced degradation

During the dark to red-light transition, PIF3 is first phosphorylated and then degraded by the 26S proteasome pathway (Park et al. 2004; Al-Sady et al. 2006). We hypothesized that B subunits may have a role in PIF3 dephosphorylation since B′α, B′β, B″α, and B″β belong to a phosphatase family. Therefore, we examined native PIF3 levels in the WT mutant and the *b″αβ/b′αβ* quadruple mutant using 4-d-old dark-grown seedlings and dark-grown seedlings exposed to red light for various times. We found that PIF3 was gradually degraded in both the WT and the *b″αβ/b′αβ* quadruple mutant after red-light treatment. However, the degradation rate of native PIF3 in the *b″αβ/b′αβ* quadruple mutant was faster than that in the WT background (Fig. 4, A and B). When we performed the PIF3 degradation assay by using the WT mutant and *b″αβ* double mutant, PIF3 also showed a faster degradation in the *b″αβ* double mutant compared with that in the WT (Supplementary Fig. S15, A and B). Conversely, PIF3 degradation was slower in the *B′α-OX* background compared with that in the WT under red light (Supplementary Fig. S15C). These data suggest that the B subunits inhibit the red-light-induced degradation of PIF3.

To test whether the phosphorylation level of PIF3 is altered in the *b″αβ* mutant compared with that in the WT, we performed an immunoblot analysis of PIF3-MYC levels in *PIF3-MYC*/Col-0 and *PIF3-MYC/cr-b″αβ* #32 backgrounds. The results showed that the phosphorylated form of PIF3-MYC had a higher relative abundance in the *PIF3-MYC/cr-b″αβ* #32 background compared with that in the *PIF3-MYC*/Col-0 transgenic lines after 20 min red-light exposure (Fig. 4, C and D; Supplementary Fig. S16A). These data suggest that B″α and B″β prevent PIF3 degradation by regulating PIF3 phosphorylation status under red light.

To examine how fast the phosphatases were acting on PIF3, we checked the PIF3-MYC phosphorylation status after 1 h red-light treatment to induce PIF3-MYC phosphorylation in the presence of Bortezomib and MG132 to inhibit its degradation, and then 5 min

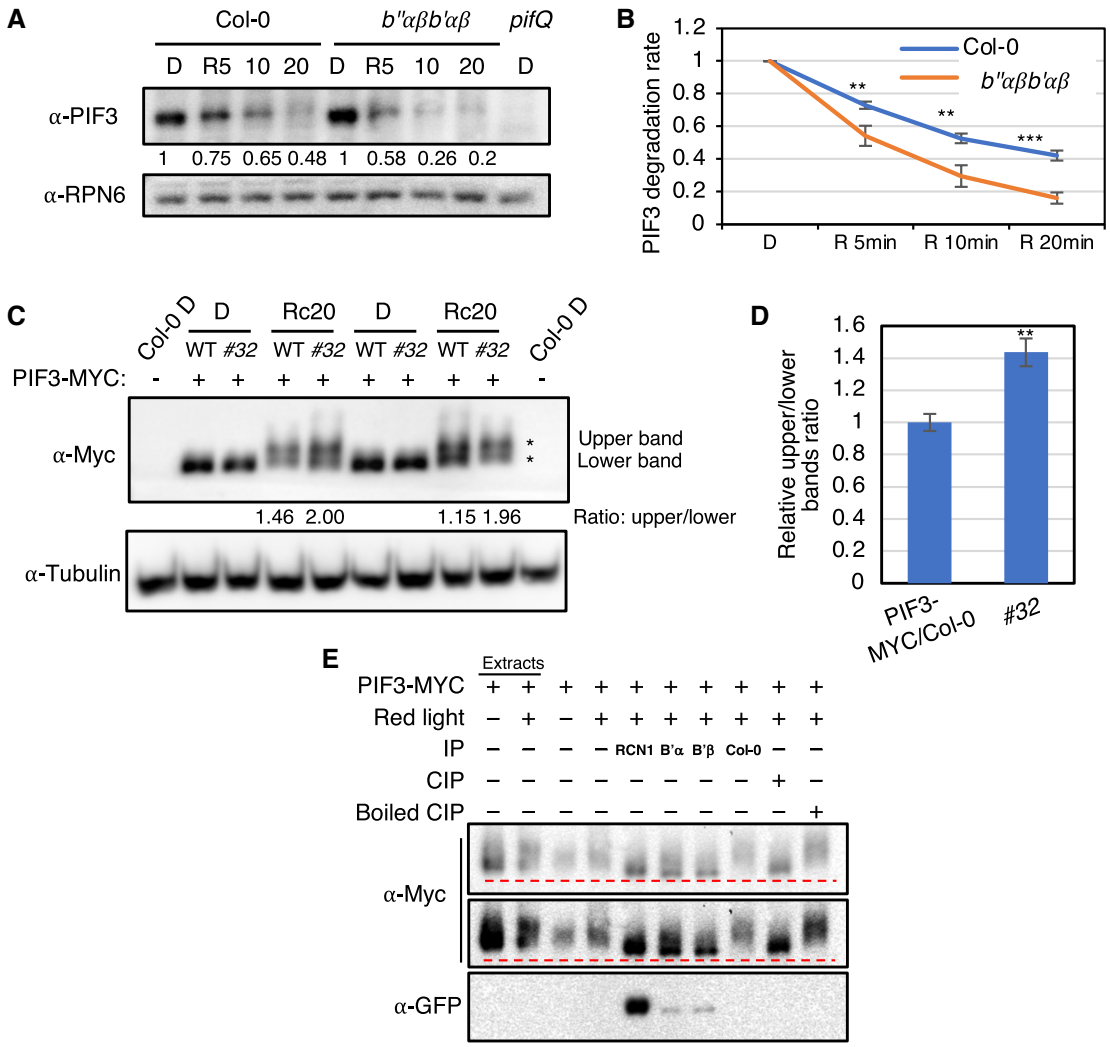

Figure 4. PP2A controls the PIF3 level under red light by dephosphorylation. **A)** Immunoblots showing the light-induced degradation of native PIF3 in the *pp2ab″αβb′αβ* mutant compared with the WT. Four-day-old dark-grown seedlings were either kept in darkness or exposed to red light (20 μmol m^{-2} s^{-1}) for the duration indicated before being sampled for protein extraction. RPN6 blot was used as the loading control. The numbers show the abundance of the native PIF3 protein after calibrating with RPN6 bands. The assay was repeated independently twice with similar results. **B)** The line graphs show the native PIF3 degradation rate after red-light exposure in the WT and *pp2ab″αβb′αβ* mutant backgrounds based on 3 independent blots. $^{**}P < 0.01$ and $^{***}P < 0.001$, based on Student's *t*-test. The error bars represent SE ($n = 3$). **C)** The immunoblots show the light-induced phosphorylation of PIF3-MYC in the *cr-b″αβ #32* mutant and the WT. Four-day-old dark-grown seedlings were treated with 100 μM Bortezomib for 4 h and then either kept in darkness or exposed to red light (20 μmol m^{-2} s^{-1}) for 20 min. Four-day-old dark-grown seedlings of WT (Col-0) samples were loaded at the first lane and last lane to keep the PIF3-MYC bands running properly. The Tubulin blot shows the loading control. The asterisks indicate the PIF3-MYC upper and lower bands in the WT and #32 mutant. The values show the ratio of the upper/lower band. **D)** A quantification of the relative PIF3-MYC upper/lower band ratio in the WT and #32 after red-light treatment in immunoblots shown in (**C**). The relative PIF3-MYC upper/lower band ratio in the WT was set as 1. $^{**}P < 0.01$, based on Student's *t*-test. The error bars represent SE ($n = 6$). **E)** PP2A dephosphorylates PIF3 in vitro. A dephosphorylation assay was performed by using immunoprecipitated PIF3-MYC and PP2A proteins from PIF3-MYC plants and RCN1-GFP, YFP-B′α, and YFP-B′β transgenic plants, respectively. PIF3-MYC proteins from 4 dark-grown seedlings of PIF3-MYC, treated with 100 μM Bortezomib for 4 h in darkness and exposed to red light before the IP process. RCN1-G, YFP-B′α, and YFP-B′β IP products as PP2A phosphatase incubate with immunoprecipitated PIF3-MYC for 1 h at 30 °C. CIP as a positive control. Boiled CIP and IP products from Col-0 as negative controls. CIP and boiled CIP treatments were performed at 37 °C for 1 h. A Western blot analysis was performed with anti-Myc on SDS–PAGE. CIP, calf intestine phosphatase; D, dark; R, red light.

far-red-light treatment to inactivate phys, followed by 5, 10, 15, and 20 min dark incubation of *PIF3-MYC*/Col-0 and *PIF3-MYC/cr-b″αβ (#32)* seedlings. We evaluated the phosphorylation level by using the ratio of the upper/lower band. We found that after 1 h red-light treatment, the ratio was similar between the WT and #32, at 2.05 or 2.04 (Supplementary Fig. S16B). In the WT background, after 5 min dark treatment, the ratio became 0.79, and after 20 min dark treatment, the ratio became 0.24 (Supplementary Fig. S16B). These data suggest that 5 min dark treatment is sufficient to induce PIF3-MYC dephosphorylation, and PIF3-MYC dephosphorylation happens fast within 20 min when the samples are kept in the dark. When we compared PIF3-MYC dephosphorylation between the WT and #32 based on the ratio, we found that PIF3-MYC dephosphorylation was slower in the #32 background than in the WT background, especially during the early time points (Supplementary Fig. S16B), which suggests that PP2A B″α and B″β are involved in dark-induced PIF3-MYC dephosphorylation. However, the dark-induced PIF3-MYC dephosphorylation is not abolished in the #32 background, suggesting that other PP2A subunits or other phosphatases are also involved in this process.

To examine whether PP2A can directly dephosphorylate PIF3 in vitro, we conducted the dephosphorylation assay using

immunoprecipitated PIF3-MYC and different PP2A subunits from *35S:PIF3-MYC*/Col-0, *PP2A 35S:A3-GFP*/Col-0, *RCN1-GFP*/Col-0, *B″β-GFP*/Col-0, *YFP-B′α*/Col-0, and *YFP-B′β*/Col-0 transgenic plants, respectively. We used the A3-GFP, RCN1-GFP, B″β-GFP, YFP-B′α, and YFP-B′β IP products as PP2A phosphatase and performed incubation with immunoprecipitated PIF3-MYC. As shown in Fig. 4E and Supplementary Figs. S15D and S17A, A3-GFP, RCN1-GFP, YFP-B′α, and YFP-B′β immunoprecipitated products can directly dephosphorylate PIF3-MYC, similar to the positive control calf intestinal phosphatase (CIP) treatment. However, the B″β-GFP immunoprecipitated products failed to dephosphorylate PIF3-MYC even in the presence of Ca^{2+} (Supplementary Fig. S17A), similar to the boiled CIP negative control. To investigate the reason for the inability of B″β-GFP to dephosphorylate PIF3-MYC, we checked whether B″β-GFP could associate with the PP2A C subunit. As shown in Supplementary Fig. S17B, only a small amount of the C subunit was found to co-precipitate with the B″β-GFP compared with RCN1-GFP, which suggests that B″β-GFP exhibits a lower binding ability to the C subunit compared with RCN1-GFP. Interestingly, YFP-B′α and YFP-B′β showed normal binding to the C subunit compared with B″β-GFP (Supplementary Fig. S18). To test whether the C-terminal GFP fusion was causing a reduced association with the C subunit, we generated the *35S:B′β-GFP*/Col-0, *35S:YFP-B″α*/Col-0, and *35S:YFP-B″β*/Col-0 transgenic plants and examined the PP2A C subunit after performing the IP from YFP-B′β, B′β-GFP, YFP- B″α, and YFP-B″β plants. In this assay, we used RCN1-GFP and YFP-B′α as positive controls and B″β-GFP as a negative control. The results showed that B′β-GFP exhibited a lower binding ability compared with YFP-B′β (Supplementary Fig. S18A). Quantitative data showed that YFP-B′α and YFP-B′β exhibited a similar strong binding ability to the C subunit among these subunits tested. However, B′β-GFP showed only a 1/3 binding ability to the C subunit compared with YFP-B′β. B″α and B″β fused to GFP or YFP at both the N-terminus and the C-terminus and displayed the lowest binding ability to the C subunit among the subunits tested (Supplementary Fig. S18, A and B). These data suggest that a free C-terminus may be essential for the B″ subunits to bind strongly to the C subunit for PP2A holoenzyme assembly, and that B″β fails to dephosphorylate PIF3-MYC, possibly due to its low affinity for the C subunit.

PP2A B″α and B″β alter gene expression in response to red light

Red light induces global changes in gene expression to regulate photomorphogenesis (Tepperman et al. 2004; Pfeiffer et al. 2014). To test whether PP2A B″α and B″β can regulate gene expression in response to red light, RNA-sequencing (RNA-seq) was conducted by using a 4-d-old dark-grown seedling of the WT and *b″αβ* mutants, kept in the dark or under 1 h of red-light (8 μmol m^{-2} s^{-1}) treatment before the samples were collected. The results showed that 1,359 genes were differentially expressed in the WT and 1,387 genes were regulated in the *b″αβ* mutant in response to 1 h of red-light exposure (Fig. 5A; Supplementary Data Set 1). In addition, 512 genes were *B″α* and *B″β* dependent, which was around 38% of the DEGs (Supplementary Data Set 1). Furthermore, 1,359 DEGs in the WT displayed different patterns in *b″αβ*, as shown in the heat map analysis (Fig. 5B). A gene ontology (GO) analysis of 512 PP2A B″α- and B″β-dependent genes showed an enrichment of the genes associated with responses to endogenous, external, osmotic, and temperature stimulus and a regulation of biological processes (Fig. 5C). Overall, these data suggest that PP2A B″α and B″β are crucial for transcriptional regulation in photomorphogenesis.

To confirm the RNA-seq data, we performed RT-qPCR assays to examine the transcript level of several red-light responsive genes, such as *MYB61*, *CBF1*, and AT5G40500 (Fig. 5D). Consistent with the RNA-seq data, the transcript levels of these genes were upregulated in response to red light in the WT background. However, the transcript levels showed either no change or were slightly upregulated after red-light treatment in *b″αβ*, and similar trends were observed in the *pif3* background. Combined with the PIF3 degradation results (Fig. 4, A and B; Supplementary Fig. S15), these data suggest that red-light-induced PIF3 degradation does affect downstream gene expression. In summary, these data indicate that PP2A B″α and B″β play an important role in photomorphogenesis via transcriptional regulation.

To determine whether PP2A and PIF3 coregulated gene expression under red light, we also compared the *b″αβ* RNA-seq data with *pif3* microarray data (Monte et al. 2004). Although these 2 datasets were generated using 2 different techniques, the Venn diagram showed that 512 DEGs were *B″αβ* dependent, 1,196 DEGs were *PIF3* dependent, and 492 DEGs were both *PIF3* and *B″αβ* dependent (Supplementary Fig. S19A). Among the *B″αβ*-dependent DEGs, 283 DEGs were upregulated, while 229 DEGs were downregulated. Similarly, among the *PIF3*-dependent DEGs, 823 DEGs were upregulated, while 373 DEGs were downregulated. The Venn diagrams showed that a majority of the *B″αβ*-dependent upregulated and downregulated DEGs overlapped with the *PIF3*-dependent upregulated and downregulated DEGs, respectively (Supplementary Fig. S19, B and C). In addition, a comparison between *B″αβ*-dependent DEGs and PIF direct target genes (DTGs; Pfeiffer et al. 2014) revealed 17 overlapping genes ($P < 2.0 \times 10^{-5}$, hypergeometric test; Supplementary Fig. S19D). The reason for the relatively few overlapping genes could possibly be attributed to the fact that PIFs were not absent in the *pp2a b″αβ* background but showed a rather modest reduction due to faster degradation compared with that in the WT under red light.

The expression and stability of PP2A subunits are modestly regulated by light

To examine the subcellular localization of the PP2A B′α, B′β, B″α and B″β subunits, we examined the YFP-B′α, YFP-B′β, YFP-B″α, and YFP-B″β localization by using *YFP-B′α/Col-0*, *YFP-B′β/Col-0*, *YFP-B″α/Col-0*, and *YFP-B″β/Col-0* lines, respectively. Strong YFP signals were found in the nucleus and cytoplasmic area of the primary root and hypocotyl cells (Fig. 6; Supplementary Fig. S20). Thus, PP2A B′ and B″ subunits might function in both nucleus and cytoplasm. To test whether the stability of the B′ and B″ subunits was regulated by light, 4-d-old dark-grown seedlings were exposed to red light for 1 and 6 h, and the protein level was examined using an anti-GFP antibody. The results showed that the abundance of the B′α and B″β subunits was modestly increased under light conditions (Fig. 7). We also performed RT-qPCR to test whether the expression of any of the PP2A subunits was regulated by light. The results showed that the expression of *B′α*, *A2*, and *C5* was slightly upregulated under red light, while the expression of the *C1* subunits was slightly reduced under 6 h of red light (Supplementary Fig. S21). Finally, we examined whether the expression of the A and C subunits was altered in the *b″αβ/b′αβ* quadruple mutant background under dark and light conditions. The results showed that the expression of *RCN1*, *A2*, *C1*, *C2*, and *C3* was not altered in the *b″αβ/b′αβ* quadruple mutant background compared with that in the WT controls (Supplementary Fig.

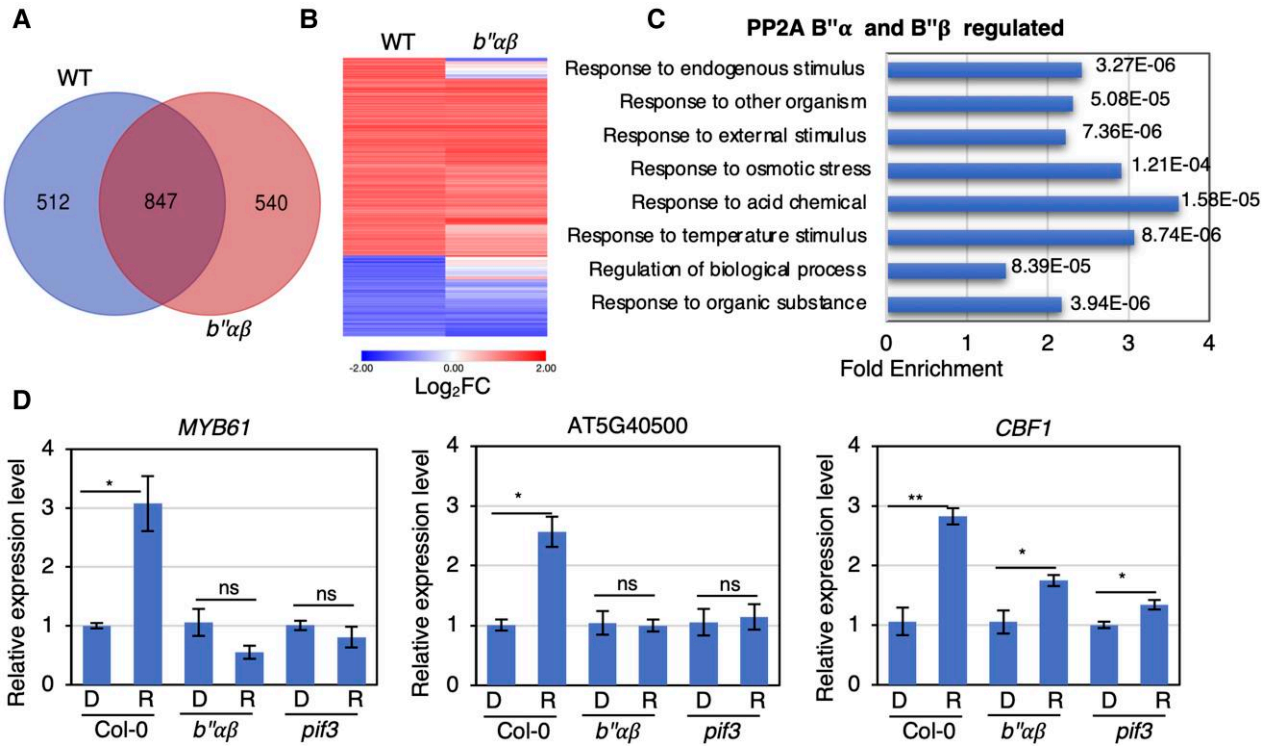

Figure 5. RNA-seq revealing unique roles of PP2A B″α and B″β in gene expression after red-light exposure. **A)** A Venn diagram shows differentially expressed genes (DEGs) in the WT vs. the *pp2ab″αβ* mutant after red-light exposure. Four-day-old dark-grown seedlings were exposed to continuous red light (20 μmol m^{-2} s^{-1}) for 1 h or kept in darkness and total RNA was extracted from 3 biological replicates for RNA-seq analyses. **B)** A hierarchical clustering from 1,359 DEGs from the WT shows a distinct pattern in the *pp2ab″αβ* mutant after red-light exposure. **C)** A GO analysis of PP2A B″α and B″β-dependent 512 genes. **D)** A RT-qPCR analysis using MYB61, AT5G40500, and CBF1. RT-qPCR samples were extracted from 4-d-old dark-grown seedlings of Col-0, *pp2ab″αβ*, and *pif3* and then were either kept in the dark or exposed to continuous red light (20 μmol m^{-2} s^{-1}) for 1 h. Three biological repeats were performed. The error bars represent SE ($n = 3$). Relative gene expression levels were normalized using the expression level of ACT2 and the values of those genes in dark conditions. Student's *t*-test was performed. *$P < 0.05$, **$P < 0.01$. D, dark; FC, fold change; R, red light.

S22). These data suggest that light signals have a modest, if any, impact on the expression and stability of the PP2A subunits.

Discussion

The reversible phosphorylation of proteins, especially transcription factors, plays crucial roles in regulating the physiology of all organisms and has been implicated in almost all signaling pathways (Stark 2004). Attachment of a phosphate by a kinase and removal of the phosphate by a phosphatase provide a reversible way of regulating the activity, abundance, and/or subcellular localization of a protein. PIFs are a group of bHLH transcription factors that function as negative regulators of photomorphogenesis. In recent years, it has been shown that PIFs are first phosphorylated by multiple kinases and then degraded through the ubiquitin/26S proteasome pathway (Cheng et al. 2021; Cai and Huq 2024). Our data and those of others show that PIF3 is also dephosphorylated by multiple phosphatases to fine-tune photomorphogenesis (Yu et al. 2019; Huq et al. 2024).

Several lines of evidence support our conclusion that PP2A regulates photomorphogenesis by dephosphorylating PIF3. First, PP2A B′α, B′β, B″α, and B″β interact with PIFs in vitro and in vivo. (Fig. 1; Supplementary Figs. S1 and S4). Second, *pp2ab″αβ* and *b″αβ/b′αβ* seedlings exhibit short hypocotyls in red-light conditions compared with the WT in a light-dependent manner (Fig. 2, A to D; Supplementary Fig. S7). Conversely, B′α, B″α, and B″β overexpression lines show longer hypocotyls compared with the WT (Fig. 2, A to D; Supplementary Fig. S7). Third, B″α, B″β, and PIF function in the same genetic pathway to regulate hypocotyl elongation (Fig. 3; Supplementary Fig. S9). Fourth, the light-induced degradation of PIF3 is faster in *b″αβ/b′αβ* and *b″αβ* compared with that in the WT background (Fig. 4, A and B; Supplementary Fig. S15, A and B). Fifth, the phosphorylation level of PIF3 under red light is higher in the *b″αβ* background compared with that in the PIF3-MYC transgenic line (Fig. 4C). Sixth, PP2A directly dephosphorylates PIF3-MYC in vitro (Fig. 4D; Supplementary Figs. S15C and S17A). Seventh, PP2A B″α and B″β regulate gene expression in response to red light (Fig. 5). Taken together, these data firmly establish that PP2A functions as a negative regulator of photomorphogenesis.

Previously, 2 phosphatases have been reported to regulate PIF phosphorylation status and abundance. The first reported phosphatase to regulate PIF stability is TOPP4, a catalytic subunit of the PP1 family (Yue et al. 2016). TOPP4 inhibits the red-light-induced ubiquitination and degradation of PIF5 during photomorphogenesis in Arabidopsis. The *topp4-1* mutant displays short hypocotyls and an expanded cotyledon compared with the WT under red light. Further, protein interaction assays and phosphorylation studies demonstrate that TOPP4 interacts directly with and dephosphorylates PIF5. However, *topp4* is isolated as a dwarf mutant, suggesting a more general function in regulating plant growth and development (Qin et al. 2014). FyPP1 and FyPP2, 2 catalytic subunits of PP6, also regulate PIFs (Yu et al. 2019). FyPP1 and FyPP2 directly interact with PIF3 and PIF4 in Arabidopsis. Although PP6 inhibits a red-light-induced degradation of PIF4, two pieces of evidence suggest that FyPP1 and FyPP2 mainly

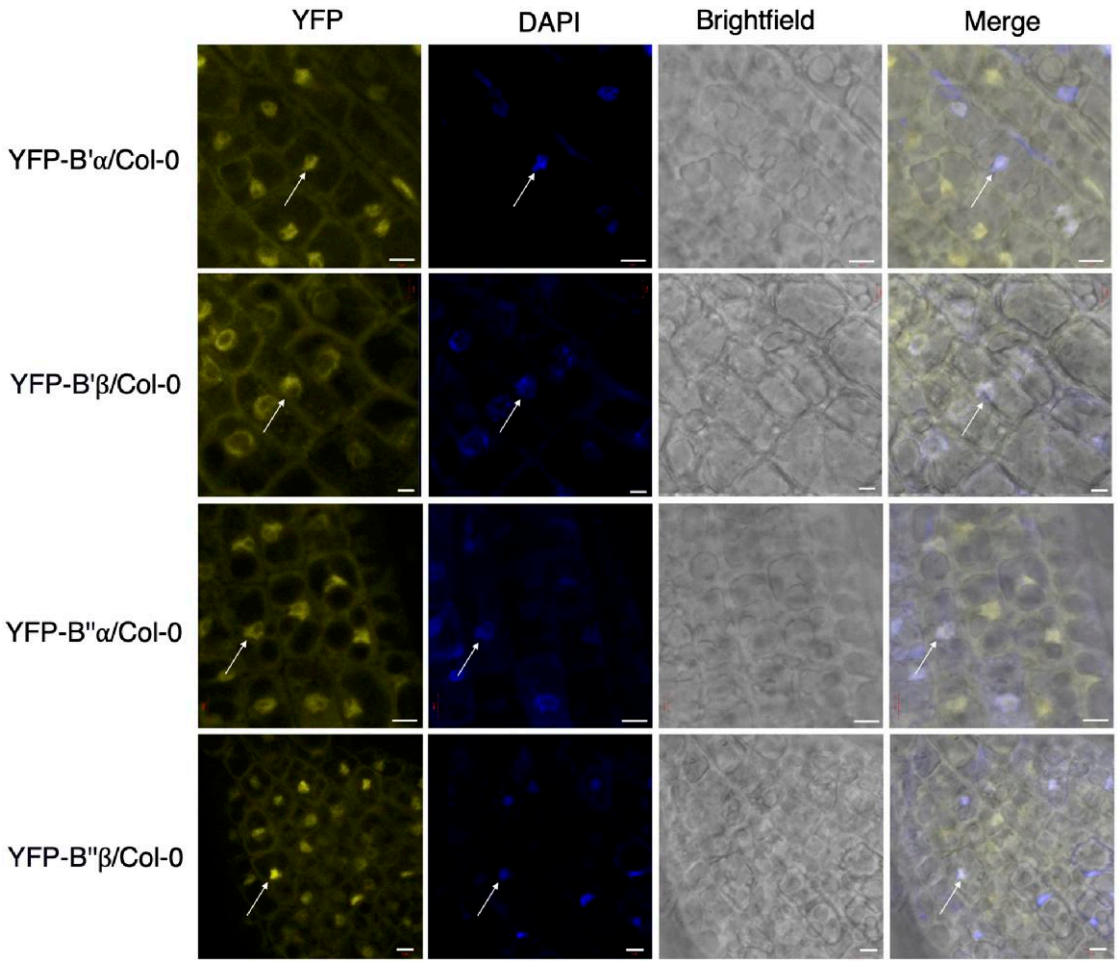

Figure 6. The B subunits are located in both the nucleus and the cytoplasm. Confocal images showing the subcellular localization of YFP-B′α, YFP-B′β, YFP-B″α, and YFP-B″β, in the primary root of 4-d-old seedlings grown on an MS medium in white light conditions. DAPI was used to show the nucleus. The white arrows show the nucleus. Scale bar is 5 μm.

function in dark conditions. First, the *fypp1* and *fypp2* mutants show short hypocotyls in the dark compared with the WT, but these are slightly longer than *pifQ*. Second, PIF3 and PIF4 proteins exhibit mobility shifts in the *fypp1* and *fypp2* mutants due to their hyperphosphorylation in dark conditions compared with that in the Col-0 background. Thus, PP2A B subunits regulate PIF stability and phosphorylation status only under light conditions, which are different from previously reported phosphatases. Based on our data, B″α and B″β are 2 PP2A regulatory subunits that specifically function in red-light conditions because *b″αβ*, *B″α-OX*, and *B″β-OX* lines only display hypocotyl phenotypes different from the WT specifically under red-light conditions (Fig. 2; Supplementary Figs. S6, A to D and S7, A to D). Interestingly, the interaction between PIF3 and PP2A B subunits is not regulated by light as they interact under both dark and light conditions (Fig. 1; Supplementary Fig. S1). However, *b″αβ*, *B″α-OX*, and *B″β-OX* lines only display phenotypes under red-light conditions, suggesting that these B subunits may preferentially dephosphorylate the light-induced phosphorylation sites in PIF3 to control PIF3 abundance.

Although our genetic and biochemical data support the conclusion that PP2A regulates photomorphogenesis by dephosphorylating PIF3, the change in the phosphorylation status of PIF3 in the *cr-b″αβ #32* background is rather modest after red-light treatment (Fig. 4C). Interestingly, PIF3-MYC dephosphorylation happens very fast. Five minutes of dark incubation are sufficient to initiate PIF3-MYC dephosphorylation (Supplementary Fig. S16B), suggesting that the phosphorylation/dephosphorylation of PIF3 is highly dynamic. PIF3 has been shown to be phosphorylated in a large number of serine/threonine residues (Ni et al. 2013). It is possible that PP2A B′ and B″ subunits dephosphorylate only a subset of these phosphorylation sites. This is consistent with our cantharidin treatment data, suggesting that other phosphatases, including the PP1 family, may also participate in the PIF3 dephosphorylation process. Identifying the exact dephosphorylation sites may help in understanding the role of PP2A B′ and B″ subunits in this process.

Although PP2A B subunits regulate photomorphogenesis, the hypersensitive phenotypes of the *b′αβ*, *b″αβ*, and *b″αβ/b′αβ* mutants are rather weak under red-light conditions. There are more than 17 B subunits in the PP2A family in Arabidopsis (Farkas et al. 2007; Booker and DeLong 2017), suggesting that the gene redundancy may contribute to the weak hypocotyl phenotypes (Fig. 2, A to D; Supplementary Figs. S6 and S7). It is highly possible that other B subunits are also involved in this process. Our pharmacological data support this conclusion where *pp2ab″αβ* and *b″αβ/b′αβ* are hyposensitive to cantharidin, but *B″α-OX* and *B″β-OX* lines are hypersensitive to cantharidin (Supplementary Figs. S13 and S14), meaning that there are other subunits and/or classes of phosphatases involved in this process. Interestingly, *pif3* is hyposensitive to cantharidin, but *PIF3-MYC* is hypersensitive to cantharidin

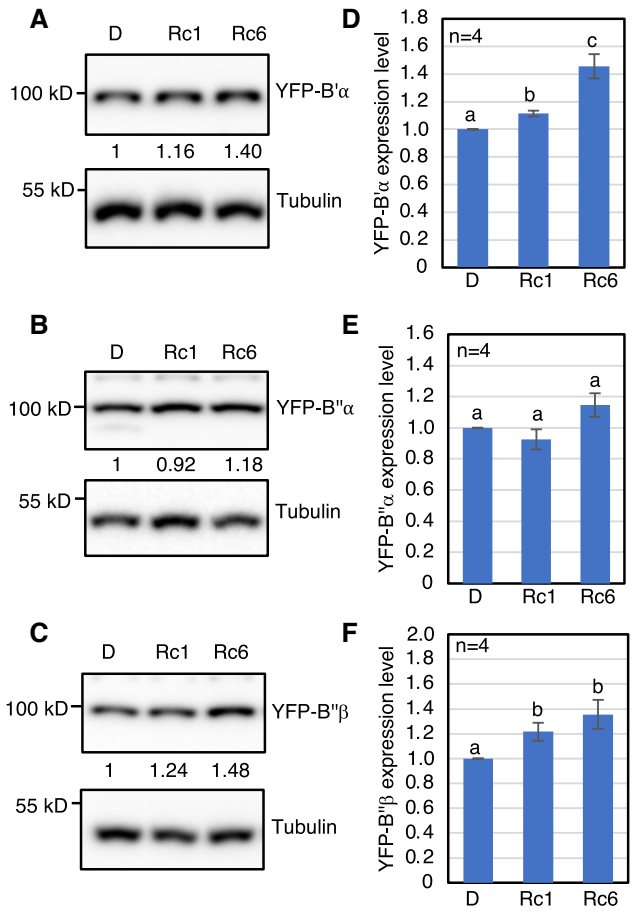

Figure 7. PP2AB′α and B″β protein levels were induced by red light. Immunoblots showing the expression of YFP-B′α (**A**), YFP-B″α (**B**), and YFP-B″β (**C**) after red-light treatment. Four-day-old dark-grown seedlings were either kept in darkness or exposed to red light (20 μmol m^{-2} s^{-1}) for 1 h (Rc1) or 6 h (Rc6) before being sampled for protein extraction. A tubulin blot was used as the loading control. The numbers show the abundance of the YFP-B′α, YFP-B″α, and YFP-B″β proteins after calibrating with Tubulin bands, respectively. The bar graphs show the expression levels of PP2AYFP-B′α (**D**), YFP-B″α (**E**), and YFP-B″β (**F**) after red-light exposure based on 4 independent blots. The error bars represent SE ($n = 4$). A one-way ANOVA analysis was performed. Statistically significant differences are indicated by different lowercase letters ($P < 0.05$). D, dark; R, red light.

(Supplementary Fig. S13), which suggests that the PIF3 function requires PP2A or PP1 family phosphatases. Overall, these data suggest that phosphatases play crucial roles in regulating PIF abundance and activity to modulate photomorphogenesis.

One unexpected finding from our co-IP assays is that a free C-terminus is essential for B′ subunits to robustly associate with C subunits in vivo. Based on our co-IP results, B′ subunits with a free C-terminus (YFP-B′α or YFP-B′β) show a stronger binding to the PP2A C subunit compared with the C-terminal fusion (B′β-GFP; Supplementary Fig. S18). These data suggest that B′ subunits promote hypocotyl elongation relying on the binding ability to the C subunit of PP2A. B″β-GFP shows modestly longer hypocotyls than the WT (Fig. 2, F and H). Even though the B″β-GFP protein level is much higher than that in YFP-B′α (Supplementary Fig. S18), *YFP-B′α* (*B′α-OX*) exhibits much longer hypocotyls compared with the WT (Supplementary Fig. S7). B″α and B″β display low affinity to the C subunit in both N- and C-terminal fusions with GFP or YFP (Supplementary Fig. S18, A and B), explaining their modest role in regulating photomorphogenesis.

B″α and B″β proteins contain an EF-hand domain, which binds to Ca^{2+} in vitro (Leivar et al. 2011). However, Ca^{2+} is not required for the interactions between PIF3 and B″α/B″β, as our semi-in vivo pull-down buffer or co-IP buffer contains EDTA, which can sequester metal ions, including Ca^{2+}. The addition of Ca^{2+} in the dephosphorylation buffer for the in vitro dephosphorylation assay does not show any effect on the dephosphorylation of PIF3-MYC (Supplementary Fig. S17A). In addition, the absence or presence of Ca^{2+} does not affect the binding ability of B″α-GFP or B″β-GFP to the PP2A C subunit. Thus, the effect of Ca^{2+} may be substrate specific for these proteins.

In summary, our data show that PP2A B subunits directly interact with PIFs and dephosphorylate PIF3 to inhibit its degradation to fine-tune photomorphogenesis. PP2A is a group of phosphatases that regulate PIF phosphorylation and stability in the photomorphogenesis process, along with other phosphatases. Thus, multiple kinases and phosphatases regulate PIF abundance and activity in order to regulate photomorphogenesis (Fig. 8).

Materials and methods

Plant growth conditions and hypocotyl phenotype analysis

All seeds were in the Arabidopsis (*A. thaliana*) Col-0 background. The T-DNA insertion mutants used in this paper were *b″α* (SALK_135978), *b″β* (SALK_151964), and *b′αβ* (Tang et al. 2011). Seeds were surface-sterilized in 1% (v/v) bleach solution with 0.3% (w/v) SDS for 10 min, followed by 5 quick rinses with sterile water, and then plated on Murashige and Skoog (MS) basal salts without sucrose. The seeds were stratified at 4 °C in the dark for 3 d, followed by white light (50 μmol m^{-2} s^{-1}) exposure for 3 h to promote germination, and then kept either in the dark (22 °C) or in continuous red light (light intensity and time of exposure indicated in each figure) for 4 d for an immunoblot analysis or a hypocotyl elongation analysis. The hypocotyl length was measured using ImageJ software and analyzed by using a 1-way ANOVA or Student's *t*-test. The monochromatic red-light sources have been described previously (Castillon et al. 2009). Statistical differences are indicated by different letters or asterisks ($P < 0.05$).

Construction of vectors and generation of transgenic plants

To generate *B″α-OX*, *B″β-OX*, *RCN1-OX*, and *A3-OX* transgenic plants, the *B″α*, *B″β*, *RCN1*, and *A3* coding sequences were amplified using primers listed in Supplementary Table S1 and subcloned into the pENTR vector (Thermo Fisher Scientific, Cat# K240020). pENTR-B′α and pENTR-B′β vectors have been previously described (Wang et al. 2016). Then, pENTR-B″α, B″β, B′β, RCN1, and A3 were recombined to the pB7FWG2 gateway binary vector with the 35S promoter (Karimi et al. 2005) and c-GFP tag by using LR Clonase II (Thermo Fisher Scientific, Cat# 11791020). Then, pB7FWG2 destination vectors with genes were transformed into the Col-0 background, and transformants were selected by using the Basta antibiotic. Homozygous transgenic plants expressing GFP fusion proteins were selected from the T3 generation with detectable GFP signals. *YFP-B′α* and *YFP-B′β* transgenic plants have been described previously (Tang et al. 2011).

To generate *crispr-b″αb″β*, 2 sets of target sites were selected from close to the N-terminus of the *B″α* and *B″β* genes. pHEE401E was chosen as a destination vector (Wang et al. 2015). Then, pHEE401E-B″αB″β was transformed into a *PIF3-MYC* background, and transformants were selected by using Hygromycin B and Kanamycin antibiotics. Homozygous lines were selected by sequencing.

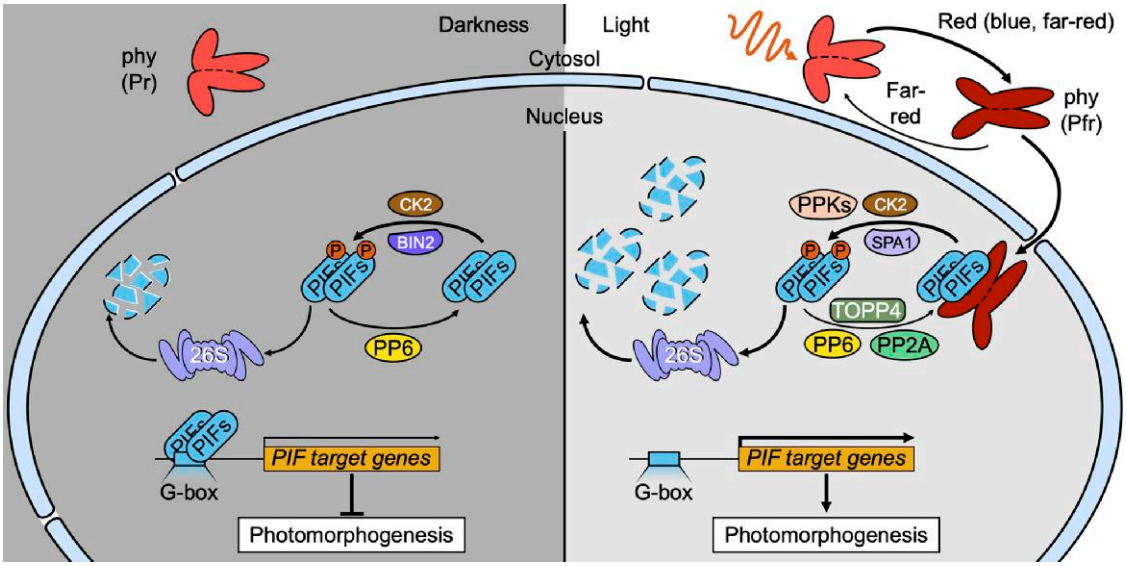

Figure 8. A model of the phy signaling pathway. (Left) In the dark, phys are in an inactive Pr form and stay in the cytosol. The nuclear-localized PIFs can form homodimers, heterodimers, or tetramers to bind to the promoter region of their target genes to repress their expression and prevent photomorphogenesis. In addition, 2 kinases (CK2 and BIN2) can phosphorylate PIFs to promote their degradation in the dark, while PP6 dephosphorylates PIFs to stabilize them, thereby inhibiting photomorphogenesis. (Right) Upon light exposure, phys convert from a Pr form to an active Pfr form and translocate into the nucleus. In the nucleus, the interaction between phys and PIFs triggers the rapid phosphorylation of PIFs by several kinases (SPA1, CK2, and PPKs). The phosphorylated PIFs will be degraded by the 26S proteasome pathway. The degradation of the PIFs promotes a light-regulated gene expression and photomorphogenesis. Conversely, PP2A with other phosphatases (TOPP4 and PP6) can dephosphorylate PIFs to inhibit their degradation to fine-tune photomorphogenesis.

Protein purification from *Escherichia coli*

For MBP-B′α, B′β, B″α, and B″β, LR reactions were performed between pENTR-B genes and the pVP13 vector with an MBP tag (Jeon et al. 2005). Each plasmid was transformed into BL21(DE3) cells. Protein expression was induced under 16 °C for 12 h with 0.1 mM Isopropyl ß-D-1-thiogalactopyranoside (IPTG). An extraction buffer [50 mM Tris, pH 7.5, 150 mM NaCl, 1 mM EDTA, 0.1% Tween 20 (v/v), 0.25 mM DTT, 1× protease inhibitor cocktail, 1 mM phenylmethylsulfonyl fluoride (PMSF)] was added to the cell pellet, which was vortexed to resuspend the cell. Sonication was performed to break the cells, and the extracts were cleared by centrifugation at 20,000×*g* for 15 min. The supernatants were incubated with amylose resin (NEB, Cat# E8021S) for 1 h in the dark at 4 °C. Amylose resin was washed with the extraction buffer 3 times for 10 min each time. The MBP protein was still bound to resin for the following in vitro pull-down assays.

Protein interaction assays

For semi-in vivo pull-down assays, 4-d-old dark-grown seedlings of 35S:*PIF3-MYC* were treated with 100 μM Bortezomib for 4 h in darkness. One batch was ground in liquid nitrogen. Another batch was exposed to 20 μmol m^{-2} s^{-1} red light for 10 s and then kept in the dark until 10 min before being ground in liquid nitrogen. Total protein was solubilized in an extraction buffer [50 mM Tris, pH 7.5, 150 mM NaCl, 1 mM EDTA, 0.1% Tween 20 (v/v), 0.25 mM DTT, 1× protease inhibitor cocktail (Sigma-Aldrich, Cat# P9599), 1 mM PMSF]. The extracts were cleared by centrifugation at 20,000×*g* for 15 min. The supernatants were incubated with beads bound with MBP-B″α, MBP-B″β, and MBP only as a control for 1 h in the dark at 4 °C. The beads were washed 3 times, 10 min each with the extraction buffer. The beads were then boiled with a 2× SDS sample buffer, and the supernatants were separated on an SDS–PAGE gel. An anti-MYC antibody (Cell Signaling, Cat# 2276S; dilution 1:5,000) was used to detect the PIF3-MYC protein.

For the in vivo co-IP assays, 4-d-old dark-grown 35S:*B″α-GFP/PIF3-MYC*, 35S:*B″β-GFP/PIF3-MYC*, 35S:*PIF3-MYC*, and Col-0 seedlings were used. 35S:*PIF3-MYC* and Col-0 were used as controls. The seedlings were treated with 100 μM Bortezomib for 4 h in darkness. One batch was ground in liquid nitrogen. Another batch was exposed to 20 μmol m^{-2} s^{-1} red light for 10 s and then kept in the dark until 10 min before being ground in liquid nitrogen. Total protein was solubilized in an extraction buffer [50 mM Tris, pH 7.5, 150 mM NaCl, 1 mM EDTA, 0.1% Tween 20 (v/v), 0.25 mM DTT, 1× protease inhibitor cocktail, 1 mM PMSF]. The extracts were cleared by centrifugation at 20,000×*g* for 15 min. The supernatants were incubated with Dynabeads bound with anti-GFP (Abcam, Cat# ab6556, 20 μL μg^{-1}) for 1 h in the dark at 4 °C. The dynabeads were washed with the extraction buffer 3 times for 10 min each time. The beads were heated to 65 °C for 15 min with a 2× SDS sample buffer and separated on an 8% SDS–PAGE gel. An anti-Myc antibody (Cell Signaling, Cat# 2276S; dilution 1:5,000) was used to detect the PIF3-MYC protein. An anti-GFP antibody (Abcam, Cat# ab6556; dilution 1:5,000) was used to detect the B″α-GFP and B″β-GFP proteins.

For the Y2H assay, AD plasmids (AD-PIF1, AD-PIF4, AD-PIF5) and BD plasmids (BD-B″α, BD-B″β) were transformed into the AH109 yeast cell simultaneously and then selected on a solid medium lacking Leu and Trp amino acids (–LT). Only successfully transformed yeast cells survive on an –LT medium. Then, these yeast cells were plated on a solid medium lacking Leu, Trp, and His amino acids (–LTH). The synthesis of His can be activated when B″α and B″β interact with PIF1, PIF4, and PIF5, and then the yeast can survive on the –LTH medium. To avoid false-positive results, 3-amino-1,2,4-triazole (3-AT) was added to the –LTH medium to inhibit the self-activation of the His synthesis.

PIF3 degradation assay

To observe native PIF3 degradation in Col-0 and *pp2ab″αβ*, 4-d-old dark-grown seedlings were used. The seedlings were exposed to

red light (20 μmol m^{-2} s^{-1}) for 0, 5, 10, and 20 min before being collected, and total protein was extracted in an extraction buffer (8 M urea, 50 mM Tris-Cl, pH 7.5, 1× protease inhibitor cocktail). An anti-PIF3 primary antibody from Agrisera (Cat# AS16 3954; dilution 1:3,000) was used, and the secondary antibody was also from Agrisera (Cat# AS09605; dilution 1:5,000). For the loading control, anti-RPT5 (Enzo Life Sciences, Cat# BML-PW8770-0025; dilution 1:5,000), anti-RPN6 (Agrisera, Cat# AS152832A; dilution 1:5,000), anti-Tubulin (Millipore Sigma, Cat# T5168; dilution 1:10,000), or Coomassie brilliant blue staining was used.

PIF3 dephosphorylation assay

IP for PIF3-MYC: Four-day-old dark-grown seedlings of PIF3-MYC were treated with 100 μM Bortezomib for 4 h in the dark and then exposed to 20 μmol m^{-2} s^{-1} red light for 10 s and then kept in the dark until 10 min before being ground in liquid nitrogen. The sample was ground in the buffer [50 mM Tris-Cl (pH = 7.5), 150 mM NaCl, 1% Triton-X 100 (v/v), 1 mM PMSF, 100 μM Bortezomib, 1× protease inhibitor cocktail, 25 mM β-glycerophosphate, 10 mM NaF, and 2 mM Na orthovanadate], and immunoprecipitated using anti-Myc (Sigma, Cat# C3956) antibody prebound to dynabeads. The immunoprecipitated PIF3-MYC was eluted with 0.1 M Glycine (pH = 2.0) from dynabeads and then neutralized with 1 M Tri-Cl (pH = 8.0; v/v = 2/1). Eluted PIF3-MYC was aliquoted into different microtubes as a substrate. *IP for PP2A*: Four-day-old dark-grown seedlings of RCN1-GFP, A3-GFP, and *b″αβ* (as a negative control) were ground in the buffer [50 mM Tris-Cl (pH = 7.5), 150 mM NaCl, 0.1% NP-40 (v/v), 1 mM PMSF, 100 μM Bortezomib, 1× protease inhibitor cocktail, 5 mM $CaCl_2$]. Samples were immunoprecipitated using an anti-GFP (Abcam, Cat# ab290) antibody prebound to dynabeads. IP products were washed once in a wash buffer [50 Tris-Cl (pH = 7.5), 150 mM NaCl, 0.1% NP-40 (v/v), 5 mM $CaCl_2$]. *Dephosphorylation*: The IP products from RCN1-GFP, A3-GFP, and *b″αβ* were mixed with the PIF3-MYC substrate in the buffer [50 mM Tris-Cl (pH = 7.5), 150 mM NaCl, 10 mM $MgCl_2$, 1 mM $MnCl_2$, 1 mM DTT, 1× protease inhibitor cocktail, 5 mM $CaCl_2$] and incubated at 30 °C in a shaker for 1 h. Quick CIP (NEB, Cat# M0525) or boiled Quick CIP was mixed with the PIF3-MYC substrate in the buffer [50 mM Tris-Cl (pH = 7.5), 100 mM NaCl, 10 mM $MgCl_2$, 1 mM DTT, 1× protease inhibitor cocktail] and incubated at 37 °C for 1 h. Immunoblotting was then performed by using 7% gel, and anti-Myc (Cell Signaling, Cat# 2276S; dilution 1:5,000) was used to detect PIF3-MYC signals.

RNA extraction, cDNA synthesis, and RT-qPCR

Four-day-old dark-grown seedlings were used with 4 independent biological replicates ($n = 4$). The seeds were surface-sterilized and plated on MS media without sucrose, cold-stratified for 3 d, and then treated for 3 h of white light. After 4 d, the seedlings were either kept in the dark or exposed to red light (20 μmol m^{-2} s^{-1}) for 1 or 6 h. Total RNA was isolated using the plant total RNA kit (Sigma, Cat# STRN250). For cDNA synthesis, 2 μg of total RNA was used for reverse transcription with M-MLV Reverse Transcriptase (Thermo Fisher Scientific, Cat# 28025013). An SYBR Green PCR master mix (Thermo Fisher Scientific, Cat# 4368577) and gene-specific oligonucleotides were used to conduct qPCR analyses using primers shown in Supplementary Table S1. Finally, the relative transcription level was calculated using the $2^{-\Delta\Delta CT}$ method, by normalizing to *ACT7*.

RNA-seq analyses

Col-0 (WT) and *pp2ab″αβ* seedlings were used for the mRNA sequence analysis. The seeds were surface-sterilized and plated on MS media without sucrose and cold-stratified for 3 d before being treated for 3 h of white light and 21 h of dark incubation to induce germination. After the initial 24 h, the seeds were further treated with far-red light (10 μmol m^{-2} s^{-1}) for 5 min to inactivate phy activity. After an additional 3 d in the dark, the seedlings were either kept in the dark (dark samples) or treated with 1 h of continuous red light (red samples; 20 μmol m^{-2} s^{-1}). Total RNA was isolated using the plant total RNA kit (Sigma, Cat# STRN250). The 3′Tag-Seq method was employed for RNA-seq analysis in this study (Lohman et al. 2016). FastQC was used for examining raw read quality (www.bioinformatics.babraham.ac.uk/projects/fastqc/). HISAT2 was used to align raw reads to the Arabidopsis genome (Kim et al. 2019). The annotation of the Arabidopsis genome was from TAIR10 (www.arabidopsis.org/). Read count data were obtained using HTseq (Anders et al. 2015; htseq.readthedocs.io/en/master/). EdgeR was used to identify the differentially expressed genes in WT/*pp2ab″αβ* (Robinson et al. 2010). The cutoff and adjusted *P*-value false discovery rate (FDR) for the differential gene expression were ≥2-fold and ≤0.05, respectively. Heat maps were generated using Morpheus (https://software.broadinstitute.org/morpheus/) and Venn diagrams were generated using the website (http://bioinformatics.psb.ugent.be/webtools/Venn/). For the heat map analysis, we used hierarchical clustering with the 1 minus cosine similarity metric combined with the average linkage method. GO enrichment analyses were performed using http://geneontology.org. GO bar graphs were generated based on the results of the significantly enriched terms with the lowest *P*-value and FDR (≤0.05) in GO terms. Raw data and processed data for RNA-seq in Col-0 and *b″αβ* can be accessed from the Gene Expression Omnibus database under accession number GSE174428.

Confocal microscopy

Root cell observation

Four-day-old seedlings grown under white light were used for subcellular localization. The samples were stained with a 1% DAPI (w/v) solution for 5 min before observation. Images were captured using a Zeiss LSM 710 inverted confocal microscope with a 63× oil objective. The image settings for DAPI were as follows: excitation light = 405 nm (intensity 8.0); pinhole = 89; gain (master) = 600; digital gain = 1.0; collection bandwidth = 410 to 470 nm. For EYFP, the image settings were as follows: excitation light = 514 nm (intensity 25.0); pinhole = 25; gain (master) = 135; digital gain = 1.0; collection bandwidth = 527 to 620 nm.

Hypocotyl cell observation

Eight-day-old seedlings grown under white light were used for subcellular localization. Water was used as the medium for observation. Images were captured using a Zeiss LSM 710 confocal microscope with a 20× objective. The image settings for EYFP were as follows: excitation light = 514 nm (intensity 25.0); pinhole = 84; gain (master) = 644; digital gain = 1.0; collection bandwidth = 527 to 620 nm.

Accession numbers

Sequence data from this article can be found in the GenBank/EMBL data libraries under accession numbers: *PIF3* (AT1G09530), *B″α* (AT5G44090), *B″β* (AT1G03960), *B′α* (AT5G03470), *B′β* (AT3G09880), *RCN1* (AT1G25490), and *A3* (AT1G13320). RNA-seq data were deposited into the Gene Expression Omnibus database (accession number GSE174428). Arabidopsis mutants and transgenic lines,

as well as plasmids and antibodies generated during the current study, are available from the corresponding author upon reasonable request.

Acknowledgments

The authors thank Dr Inyup Paik for helpful discussions and suggestions and the members of the Huq laboratory for a critical reading of the manuscript. The authors acknowledge the Texas Advanced Computing Center at The University of Texas at Austin for providing high-performance computing, visualization, and database resources that have contributed to the research results reported in this paper.

Author contributions

E.H. and X.C. conceived the study, designed the experiments, and wrote the article. X.C. carried out the experiments. S.L. and X.C. analyzed the RNA-seq data. W.T. and Y.S. helped prepare the PP2A genetic materials and Y2H vectors. S.L., Y.S., and W.T. presented their comments and edited the manuscript.

Supplementary data

The following materials are available in the online version of this article.

Supplementary Figure S1. PIF3 interacts with PP2A B′α and B′β in vivo and in vitro.

Supplementary Figure S2. An amino acid sequence alignment among PP2A B subunits.

Supplementary Figure S3. PIF3 does not interact with PP2A A subunits and catalytic C subunits in yeast.

Supplementary Figure S4. PIF1, 4, and 5 interact with PP2A B″α and B″β.

Supplementary Figure S5. The characterization of the T-DNA insertional mutants.

Supplementary Figure S6. *pp2ab″α* and *b″β* seedlings show short hypocotyls in red-light conditions.

Supplementary Figure S7. PP2A B′α and B′β promote hypocotyl elongation in red-light conditions.

Supplementary Figure S8. PP2A RCN1 and A3 overexpression seedlings show longer hypocotyls in red-light conditions.

Supplementary Figure S9. The validation of *cr-pif3* lines and phenotypic analyses under dark and red light conditions.

Supplementary Figure S10. The characterization of B″ overexpression lines.

Supplementary Figure S11. Mutation sites in *cr-b″αβ/PIF3-MYC#32*.

Supplementary Figure S12. *cr-b″αβ/PIF3-MYC#32* seedlings show short hypocotyls compared with PIF3-MYC in red-light conditions.

Supplementary Figure S13. The impact of Cantharidin on Col-0, *pp2ab″αβ*, *pif3*, PIF3-MYC, B″α-OX/Col-0, and B″β-OX/Col-0 hypocotyl elongation in red-light conditions.

Supplementary Figure S14. The impact of Cantharidin on Col-0, *pp2ab″αβ*, *b″αβ/b′αβ*, and *pifQ* hypocotyl elongation in red-light conditions.

Supplementary Figure S15. The PP2A B subunits control the PIF3 level by directly dephosphorylating PIF3 under red light conditions.

Supplementary Figure S16. PP2A regulates PIF3-MYC phosphorylation status after red-light treatment, followed by dark treatment.

Supplementary Figure S17. B″β-GFP fails to dephosphorylate PIF3-MYC in vitro and exhibits a lower binding ability with the PP2A c subunit compared with RCN1-GFP.

Supplementary Figure S18. A free C-terminus is essential for B′ subunits to bind the PP2A catalytic subunit strongly.

Supplementary Figure S19. A comparison of PP2A-regulated genes and PIF-DTGs.

Supplementary Figure S20. A subcellular localization of the B subunits of PP2A.

Supplementary Figure S21. The relative expression of different subunits of *PP2A* in Col-0 after red-light exposure.

Supplementary Figure S22. The relative expression of *PP2A* A subunits and C subunits in *b″αβ/b′αβ* after red-light exposure.

Supplementary Table S1. The primers used in this study.

Supplementary Data Set 1. An RNA-seq data analysis to identify PP2A B″αβ-subunit-regulated genes and a comparison with PIF3-regulated genes.

Funding

This work was supported by grants to E.H. from the National Science Foundation (MCB-2014408) and an Integrative Biology Research Fellowship grant to X.C. from The University of Texas at Austin

Conflict of interest statement. None declared.

Data availability

RNA sequencing data were deposited into the Gene Expression Omnibus database (accession number GSE174428). Arabidopsis mutants and transgenic lines, as well as plasmids and antibodies generated during the current study are available from the corresponding author upon reasonable request.

References

Al-Sady B, Ni W, Kircher S, Schäfer E, Quail PH. Photoactivated phytochrome induces rapid PIF3 phosphorylation prior to proteasome-mediated degradation. *Mol Cell*. 2006:23(3):439–446. https://doi.org/10.1016/j.molcel.2006.06.011

Anders S, Pyl PT, Huber W. HTSeq—a Python framework to work with high-throughput sequencing data. *Bioinformatics*. 2015:31(2):166–169. https://doi.org/10.1093/bioinformatics/btu638

Bae G, Choi G. Decoding of light signals by plant phytochromes and their interacting proteins. *Annu Rev Plant Biol*. 2008:59(1):281–311. https://doi.org/10.1146/annurev.arplant.59.032607.092859

Bernardo-García S, de Lucas M, Martínez C, Espinosa-Ruiz A, Daviere J-M, Prat S. BR-dependent phosphorylation modulates PIF4 transcriptional activity and shapes diurnal hypocotyl growth. *Genes Dev*. 2014:28(15):1681–1694. https://doi.org/10.1101/gad.243675.114

Bheri M, Mahiwal S, Sanyal SK, Pandey GK. Plant protein phosphatases: what do we know about their mechanism of action? *FEBS J*. 2021:288(3):756–785. https://doi.org/10.1111/febs.15454

Booker MA, DeLong A. Atypical protein phosphatase 2A gene families do not expand via paleopolyploidization. *Plant Physiol*. 2017:173(2):1283–1300. https://doi.org/10.1104/pp.16.01768

Bu Q, Castillon A, Chen F, Zhu L, Huq E. Dimerization and blue light regulation of PIF1 interacting bHLH proteins in Arabidopsis. *Plant Mol Biol*. 2011a:77(4–5):501–511. https://doi.org/10.1007/s11103-011-9827-4

Bu Q, Zhu L, Yu L, Dennis M, Lu X, Person M, Tobin E, Browning K, Huq E. Phosphorylation by CK2 enhances the rapid light-induced degradation of PIF1. *J Biol Chem*. 2011b:286(14):12066–12074. https://doi.org/10.1074/jbc.M110.186882

Cai X, Huq E. Shining light on plant growth: recent insights into phytochrome interacting factors. *J Exp Bot*. 2024:erae276. In press. https://doi.org/10.1093/jxb/erae276

Castillon A, Shen H, Huq E. Phytochrome interacting factors: central players in phytochrome-mediated light signaling networks. *Trends Plant Sci*. 2007:12(11):514–521. https://doi.org/10.1016/j.tplants.2007.10.001

Castillon A, Shen H, Huq E. Blue light induces degradation of the negative regulator phytochrome interacting factor 1 to promote photomorphogenic development of Arabidopsis seedlings. *Genetics*. 2009:182(1):161–171. https://doi.org/10.1534/genetics.108.099887

Cheng M-C, Kathare PK, Paik I, Huq E. Phytochrome signaling networks. *Annu Rev Plant Biol*. 2021:72(1):217–244. https://doi.org/10.1146/annurev-arplant-080620-024221

Choi G, Yi H, Lee J, Kwon YK, Soh MS, Shin B, Luka Z, Hahn TR, Song PS. Phytochrome signalling is mediated through nucleoside diphosphate kinase 2. *Nature*. 1999:401(6753):610–613. https://doi.org/10.1038/44176

Dong J, Ni W, Yu R, Deng XW, Chen H, Wei N. Light-dependent degradation of PIF3 by SCF-EBF1/2 promotes a photomorphogenic response in Arabidopsis. *Curr Biol*. 2017:27(16):2420–2430. https://doi.org/10.1016/j.cub.2017.06.062

Farkas I, Dombrádi V, Miskei M, Szabados L, Koncz C. Arabidopsis PPP family of serine/threonine phosphatases. *Trends Plant Sci*. 2007:12(4):169–176. https://doi.org/10.1016/j.tplants.2007.03.003

Han R, Ma L, Lv Y, Qi L, Peng J, Li H, Zhou Y, Song P, Duan J, Li J, et al. SALT OVERLY SENSITIVE2 stabilizes phytochrome-interacting factors PIF4 and PIF5 to promote Arabidopsis shade avoidance. *Plant Cell*. 2023:35(8):2972–2996. https://doi.org/10.1093/plcell/koad119

Honkanen RE. Cantharidin, another natural toxin that inhibits the activity of serine/threonine protein phosphatases types 1 and 2A. *FEBS lett*. 1993:330(3):283–286. https://doi.org/10.1016/0014-5793(93)80889-3

Huq E, Lin C, Quail PH. Light signaling in plants—a selective history. *Plant Physiol*. 2024:195(1):213–231. https://doi.org/10.1093/plphys/kiae110

Jeon W, Aceti D, Bingman C, Vojtik F, Olson A, Ellefson J, McCombs J, Sreenath H, Blommel P, Seder K, et al. High-throughput purification and quality assurance of Arabidopsis thaliana proteins for eukaryotic structural genomics. *J Struct Funct Genomics*. 2005:6(2–3):143–147. https://doi.org/10.1007/s10969-005-1908-7

Karimi M, Meyer BD, Hilson P. Modular cloning in plant cells. *Trends Plant Sci*. 2005:10(3):103–105. https://doi.org/10.1016/j.tplants.2005.01.008

Kim D, Paggi JM, Park C, Bennett C, Salzberg SL. Graph-based genome alignment and genotyping with HISAT2 and HISAT-genotype. *Nat Biotechnol*. 2019:37(8):907–915. https://doi.org/10.1038/s41587-019-0201-4

Kim D-H, Kang J-G, Yang S-S, Chung K-S, Song P-S, Park C-M. A phytochrome-associated protein phosphatase 2A modulates light signals in flowering time control in Arabidopsis. *Plant Cell*. 2002:14(12):3043–3056. https://doi.org/10.1105/tpc.005306

Kim J, Yi H, Choi G, Shin B, Song PS, Choi G. Functional characterization of phytochrome interacting factor 3 in phytochrome-mediated light signal transduction. *Plant Cell*. 2003:15(10):2399–2407. https://doi.org/10.1105/tpc.014498

Kim JI, Shen Y, Han YJ, Park JE, Kirchenbauer D, Soh MS, Nagy F, Schäfer E, Song PS. Phytochrome phosphorylation modulates light signaling by influencing the protein-protein interaction. *Plant Cell*. 2004:16(10):2629–2640. https://doi.org/10.1105/tpc.104.023879

Lee N, Choi G. Phytochrome-interacting factor from Arabidopsis to liverwort. *Curr Opin Plant Biol*. 2017:35:54–60. https://doi.org/10.1016/j.pbi.2016.11.004

Legris M, Ince YÇ, Fankhauser C. Molecular mechanisms underlying phytochrome-controlled morphogenesis in plants. *Nat Commun*. 2019:10(1):5219. https://doi.org/10.1038/s41467-019-13045-0

Leivar P, Antolín-Llovera M, Ferrero S, Closa M, Arró M, Ferrer A, Boronat A, Campos N. Multilevel control of Arabidopsis 3-hydroxy-3-methylglutaryl coenzyme A reductase by protein phosphatase 2A. *Plant Cell*. 2011:23(4):1494–1511. https://doi.org/10.1105/tpc.110.074278

Leivar P, Quail PH. PIFs: pivotal components in a cellular signaling hub. *Trends Plant Sci*. 2011:16(1):19–28. https://doi.org/10.1016/j.tplants.2010.08.003

Ling J-J, Li J, Zhu D, Deng XW. Noncanonical role of Arabidopsis COP1/SPA complex in repressing BIN2-mediated PIF3 phosphorylation and degradation in darkness. *Proc Natl Acad Sci U S A*. 2017:114(13):3539–3544. https://doi.org/10.1073/pnas.1700850114

Lohman BK, Weber JN, Bolnick DI. Evaluation of TagSeq, a reliable low-cost alternative for RNAseq. *Mol Ecol Resour*. 2016:16(6):1315–1321. https://doi.org/10.1111/1755-0998.12529

Luan S. Protein phosphatases in plants. *Annu Rev Plant Biol*. 2003:54(1):63–92. https://doi.org/10.1146/annurev.arplant.54.031902.134743

Ma L, Han R, Yang Y, Liu X, Li H, Zhao X, Li J, Fu H, Huo Y, Sun L, et al. Phytochromes enhance SOS2-mediated PIF1 and PIF3 phosphorylation and degradation to promote Arabidopsis salt tolerance. *Plant Cell*. 2023:35(8):2997–3020. https://doi.org/10.1093/plcell/koad117

Medzihradszky M, Bindics J, Ádám É, Viczián A, Klement É, Lorrain S, Gyula P, Mérai Z, Fankhauser C, Medzihradszky KF, et al. Phosphorylation of phytochrome B inhibits light-induced signaling via accelerated dark reversion in Arabidopsis. *Plant Cell*. 2013:25(2):535–544. https://doi.org/10.1105/tpc.112.106898

Monte E, Tepperman JM, Al-Sady B, Kaczorowski KA, Alonso JM, Ecker JR, Li X, Zhang Y, Quail PH. The phytochrome-interacting transcription factor, PIF3, acts early, selectively, and positively in light-induced chloroplast development. *Proc Natl Acad Sci U S A*. 2004:101(46):16091–16098. https://doi.org/10.1073/pnas.0407107101

Ni W, Xu S-L, Chalkley RJ, Pham TND, Guan S, Maltby DA, Burlingame AL, Wang Z-Y, Quail PH. Multisite light-induced phosphorylation of the transcription factor PIF3 is necessary for both its rapid degradation and concomitant negative feedback modulation of photoreceptor phyB levels in Arabidopsis. *Plant Cell*. 2013:25(7):2679–2698. https://doi.org/10.1105/tpc.113.112342

Ni W, Xu S-L, González-Grandío E, Chalkley RJ, Huhmer AFR, Burlingame AL, Wang Z-Y, Quail PH. PPKs mediate direct signal transfer from phytochrome photoreceptors to transcription factor PIF3. *Nat Commun*. 2017:8(1):15236. https://doi.org/10.1038/ncomms15236

Ni W, Xu S-L, Tepperman JM, Stanley DJ, Maltby DA, Gross JD, Burlingame AL, Wang Z-Y, Quail PH. A mutually assured destruction mechanism attenuates light signaling in Arabidopsis. *Science*. 2014:344(6188):1160–1164. https://doi.org/10.1126/science.1250778

Nito K, Wong CC, Yates JR 3rd, Chory J. Tyrosine phosphorylation regulates the activity of phytochrome photoreceptors. *Cell Rep*. 2013:3(6):1970–1979. https://doi.org/10.1016/j.celrep.2013.05.006

Paik I, Chen F, Ngoc Pham V, Zhu L, Kim J-I, Huq E. A phyB-PIF1-SPA1 kinase regulatory complex promotes photomorphogenesis in Arabidopsis. *Nat Commun*. 2019:10(1):4216. https://doi.org/10.1038/s41467-019-12110-y

Park E, Kim J, Lee Y, Shin J, Oh E, Chung WI, Liu JR, Choi G. Degradation of phytochrome interacting factor 3 in phytochrome-mediated light signaling. *Plant Cell Physiol*. 2004:45(8):968–975. https://doi.org/10.1093/pcp/pch125

Park E, Kim Y, Choi G. Phytochrome B requires PIF degradation and sequestration to induce light responses across a wide range of light conditions. *Plant Cell*. 2018:30(6):1277–1292. https://doi.org/10.1105/tpc.17.00913

Park E, Park J, Kim J, Nagatani A, Lagarias JC, Choi G. Phytochrome B inhibits binding of phytochrome-interacting factors to their target promoters. *Plant J*. 2012:72(4):537–546. https://doi.org/10.1111/j.1365-313X.2012.05114.x

Pfeiffer A, Shi H, Tepperman JM, Zhang Y, Quail PH. Combinatorial complexity in a transcriptionally-centered signaling hub in Arabidopsis. *Mol Plant*. 2014:7(11):1598–1618. https://doi.org/10.1093/mp/ssu087

Pham VN, Kathare PK, Huq E. Dynamic regulation of PIF5 by COP1-SPA complex to optimize photomorphogenesis in Arabidopsis. *Plant J*. 2018a:96(2):260–273. https://doi.org/10.1111/tpj.14074

Pham VN, Kathare PK, Huq E. Phytochromes and phytochrome interacting factors. *Plant Physiol*. 2018b:176(2):1025–1038. https://doi.org/10.1104/pp.17.01384

Phee BK, Kim JI, Shin DH, Yoo J, Park KJ, Han YJ, Kwon YK, Cho MH, Jeon JS, Bhoo SH, et al. A novel protein phosphatase indirectly regulates phytochrome-interacting factor 3 via phytochrome. *Biochem J*. 2008:415(2):247–255. https://doi.org/10.1042/BJ20071555

Qin Q, Wang W, Guo X, Yue J, Huang Y, Xu X, Li J, Hou S. Arabidopsis DELLA protein degradation is controlled by a type-one protein phosphatase, TOPP4. *PLoS Genet*. 2014:10(7):e1004464. https://doi.org/10.1371/journal.pgen.1004464

Robinson MD, McCarthy DJ, Smyth GK. Edger: a bioconductor package for differential expression analysis of digital gene expression data. *Bioinformatics*. 2010:26(1):139–140. https://doi.org/10.1093/bioinformatics/btp616

Ryu JS, Kim JI, Kunkel T, Kim BC, Cho DS, Hong SH, Kim SH, Fernandez AP, Kim Y, Alonso JM, et al. Phytochrome-specific type 5 phosphatase controls light signal flux by enhancing phytochrome stability and affinity for a signal transducer. *Cell*. 2005:120(3):395–406. https://doi.org/10.1016/j.cell.2004.12.019

Stark M. Protein phosphorylation and dephosphorylation. In: StarkMJR, editor. *The metabolism and molecular physiology of Saccharomyces cerevisiae*. London, UK: Taylor & Francis Group; 2004. p. 284–375.

Tang W, Yuan M, Wang R, Yang Y, Wang C, Oses-Prieto JA, KimT-W, Zhou H-W, Deng Z, Gampala SS, et al. PP2A activates brassinosteroid-responsive gene expression and plant growth by dephosphorylating BZR1. *Nat Cell Biol*. 2011:13(2):124–131. https://doi.org/10.1038/ncb2151

Tepperman JM, Hudson ME, Khanna R, Zhu T, Chang SH, Wang X, Quail PH. Expression profiling of phyB mutant demonstrates substantial contribution of other phytochromes to red-light-regulated gene expression during seedling de-etiolation. *Plant J*. 2004:38(5):725–739. https://doi.org/10.1111/j.1365-313X.2004.02084.x

Wang R, Liu M, Yuan M, Oses-Prieto JA, Cai X, Sun Y, Burlingame AL, Wang Z-Y, Tang W. The brassinosteroid-activated BRI1 receptor kinase is switched off by dephosphorylation mediated by cytoplasm-localized PP2A B′ subunits. *Mol Plant*. 2016:9(1):148–157. https://doi.org/10.1016/j.molp.2015.10.007

Wang Z-P, Xing H-L, Dong L, Zhang H-Y, Han C-Y, Wang X-C, Chen Q-J. Egg cell-specific promoter-controlled CRISPR/Cas9 efficiently generates homozygous mutants for multiple target genes in Arabidopsis in a single generation. *Genome Biol*. 2015:16(1):144. https://doi.org/10.1186/s13059-015-0715-0

Xin X, Chen W, Wang B, Zhu F, Li Y, Yang H, Li J, Ren D. Arabidopsis MKK10-MPK6 mediates red-light-regulated opening of seedling cotyledons through phosphorylation of PIF3. *J Exp Bot*. 2018:69(3):423–439. https://doi.org/10.1093/jxb/erx418

Yoo CY, He J, Sang Q, Qiu Y, Long L, Kim RJA, Chong EG, Hahm J, Morffy N, Zhou P, et al. Direct photoresponsive inhibition of a p53-like transcription activation domain in PIF3 by Arabidopsis phytochrome B. *Nat Commun*. 2021:12(1):5614. https://doi.org/10.1038/s41467-021-25909-5

Yu X, Dong J, Deng Z, Jiang Y, Wu C, Qin X, Terzaghi W, Chen H, Dai M, Deng XW. Arabidopsis PP6 phosphatases dephosphorylate PIF proteins to repress photomorphogenesis. *Proc Natl Acad Sci U S A*. 2019:116(40):20218–20225. https://doi.org/10.1073/pnas.1907540116

Yue J, Qin Q, Meng S, Jing H, Gou X, Li J, Hou S. TOPP4 regulates the stability of PHYTOCHROME INTERACTING FACTOR5 during photomorphogenesis in Arabidopsis. *Plant Physiol*. 2016:170(3):1381–1397. https://doi.org/10.1104/pp.15.01729

Zhu L, Bu Q, Xu X, Paik I, Huang X, Hoecker U, Deng XW, Huq E. CUL4 forms an E3 ligase with COP1 and SPA to promote light-induced degradation of PIF1. *Nat Commun*. 2015:6(1):7245. https://doi.org/10.1038/ncomms8245